N O T I C E

THIS DOCUMENT HAS BEEN REPRODUCED FROM MICROFICHE. ALTHOUGH IT IS RECOGNIZED THAT CERTAIN PORTIONS ARE ILLEGIBLE, IT IS BEING RELEASED IN THE INTEREST OF MAKING AVAILABLE AS MUCH INFORMATION AS POSSIBLE

NASA

Technical Memorandum 82009

A Stochastic-Dynamic Model for Global Atmospheric Mass Field Statistics

M. Ghil
R. Balgovind
E. Kalnay-Rivas

January 1981

(NASA-TM-82009) A STOCHASTIC-DYNAMIC MODEL FOR GLOBAL ATMOSPHERIC MASS FIELD STATISTICS (NASA) 62 p HC A04/MF A01 CSCL 04A

N81-19678

Unclas
G3/46 18829

Laboratory for Atmospheric Sciences
Modeling and Simulation Facility

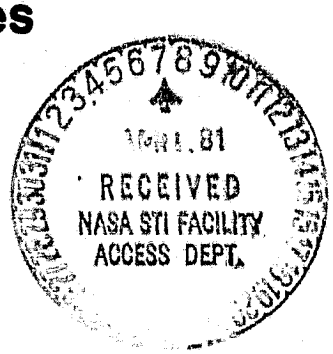

National Aeronautics and
Space Administration

Goddard Space Flight Center
Greenbelt, Maryland 20771

A STOCHASTIC-DYNAMIC MODEL FOR GLOBAL ATMOSPHERIC MASS FIELD STATISTICS

M. Ghil

Courant Institute of Mathematical Sciences
New York University, New York
and
Laboratory for Atmospheric Sciences

R. Balgovind

Sigma Data Services Corporation

E. Kalnay-Rivas

Laboratory for Atmospheric Sciences

JANUARY 1981

National Aeronautics and Space Administration
Goddard Space Flight Center
Greenbelt, Maryland 20771

Abstract

A model that yields the spatial correlation structure of atmospheric mass field forecast errors has been developed. The model is governed by the potential vorticity equation forced by random noise:

$$(\nabla^2 - c_o \sin^2\theta)\ \phi\ (\lambda,\theta;\omega) = F(\lambda,\theta;\omega) \qquad (1)$$

where ∇^2 is the Laplacian operator on the unit sphere, λ and θ are longitude and latitude, ϕ is the geopotential error field at 500mb and F is white noise corresponding to a random realization ω. The spatial covariance function Γ is defined by

$$\Gamma(\lambda_1,\theta;\lambda_2,\theta_2) = E\ \{\phi\ (\lambda_1,\theta_1;\omega)\ \phi\ (\lambda_2,\theta_2;\omega)\}, \qquad (2)$$

where E is the expected value.

Three methods of solution have been tested. In the first method, Eq. (1) was solved by expansion in spherical harmonics and the correlation function was computed analytically using the expansion coefficients. In the second method, the finite-difference equivalent of Eq. (1) was solved using a Fast Poisson Solver. The correlation function was computed using stratified sampling of the individual realizations of $F(\omega)$ and hence of $\phi\ (\omega)$. In the third method, a higher-order equation for Γ was derived from Eq. (1) and solved directly in finite differences by two successive applications of the Fast Poisson Solver. The three methods were compared for accuracy and efficiency, and the third method was chosen as clearly superior.

The results agree well with the latitude dependence of observed atmospheric correlation data. The value of the parameter c_o which gives the best fit to the data is close to the value expected from dynamical considerations. These results provide the basis for an optimal choice of coefficients for statistical analysis of atmospheric data.

Table of Contents

1. Introduction

The statistical structure of large-scale atmospheric fields is of both theoretical and practical interest to meteorologists. Theoretically, it is of interest to know what this structure is and how it becomes established (Gandin, 1963). In particular, the connection between the atmosphere's dynamics and its statistics is an attractive area of study.

Practically, numerical weather prediction (NWP) requires the accurate, detailed description of atmospheric fields as a starting point for their forecasting. The data available for such description are nonuniformly distributed in space and contaminated by various errors (Bengtsson, 1975). It is necessary, therefore, to use some form of interpolation to derive field values at the points of a uniform grid. It is desirable, furthermore, that these values be as free of errors as possible.

Interpolation coefficients can be chosen which will minimize, under certain assumptions, the expected value of the interpolation error, given the statistical properties of the errors in the data (Rutherford, 1972). This statistical approach to meteorological interpolation has become increasingly attractive recently, due to the large number of different data sources with varying error characteristics made available by the Global Atmospheric Research Program (GARP) (Fleming et al., 1979). It is often referred to as "optimal interpolation" (OI) and has been implemented operationally by the U.S. National Meteorological Center (NMC: McPherson et al., 1979), among others.

The optimal choice of interpolation coefficients in OI clearly depends on knowing the statistical properties of the fields one wishes to interpolate. Hence the practical importance of an accurate model for large-scale atmospheric statistics. The purpose of this report is to contribute to the formulation and validation of a dynamically based model for atmospheric statistics.

In a study on the use of satellite-derived temperatures for NWP, Ghil et al. (1979: to be referred to as GHA) were led to consider the difference between the observed atmospheric temperatures, T^o, and model-forecast temperatures, T^f. The model used in that study was the nine-level 4° lat. x 5° long., primitive equation, spatially second-order model of the Laboratory for Atmospheric Sciences of NASA's Goddard Space Flight Center (GLAS); temperature data were obtained from the Data System Test DST-6 held during January-March 1976.

The spatial correlations of the difference field $T^o - T^f$ were computed. It turned out that, for the same spherical distances s between points, correlations were typically higher in the tropics than in high latitudes. In other words, the correlation $\Gamma(\xi,\eta)$ of temperatures $T^o - T^f$ at a point ξ on the Earth with those at a point η a distance s away, $s = \text{dist}\,(\xi,\eta)$, falls off more rapidly with s the higher the latitude of the point ξ (Figs. 2a-d, GHA). No large or systematic dependence on height was observed when stratifying the correlations by pressure level rather than by latitude.

It was suggested (ibid.) that this striking latitude dependence of the studied field's second-order moments reflects the dependence on latitude of the Rossby radius of deformation, L. The latter is a characteristic length scale for a number of dynamic phenomena which determine the spatial structure of atmospheric fields. We decided to pursue this heuristic suggestion further, and formulated the stochastic-dynamic model investigated in this report.

Section 2 presents the model, and the governing equation, Eq. (2.7). This equation is solved by a series expansion in Section 3. For given, fixed right-hand side, Eq. (2.7) can be solved numerically by the use of a generalized Fast Poisson solver, as shown in Section 4. The full stochastic form of (2.7) is solved by Monte-Carlo simulation in Section 5. An equation for the covariance funtion $\Gamma(\xi_1, \xi_2)$ of the solution to (2.7) is derived in Section 6. It is seen to depend on a scale parameter, c_0,

$$\Gamma = \Gamma(\xi_1, \xi_2; c_0) \ .$$

Comparing model correlations with observed mass field correlations, we obtained the best value of c_0. Numerical results are presented in Section 7. Concluding remarks follow in Section 8.

2. Dynamical model of the forecast error field

We will assume that for periods of a few days, the dynamics of the atmosphere are approximately governed by the equation of conservation of potential vorticity

$$\frac{d}{dt}\left(a^{-2} \nabla^2 \psi - L^{-2} \psi + f\right) = Q. \qquad (2.1)$$

Here $\psi = \Phi / f_o$ is the quasi-geostrophic stream function, Φ being the height h of the 500mb surface multiplied by the gravity g, $\Phi = gh$; the Coriolis parameter is $f = 2 \Omega \sin \theta$, with Ω the angular velocity of rotation of the earth and θ is latitude, while f_o is a constant value of f corresponding to a mid-latitude θ_o. The radius of the earth is a, ∇^2 is the Laplacian operator on the unit sphere, with λ longitude, L is the Rossby radius of deformation, $L^2 = gD/f^2$, with D a characteristic depth. The forcing term Q represents diabatic heating, dissipation and lower-boundary effects.

Equation (2.1), with Q=0, is strictly valid for a quasi-geostrophic, frictionless, shallow-water model without topography, with a mean depth D. It is also valid for each of the vertical modes in a linearized quasigeostrophic model in which the vertical dependence has been separated out (Phillips, 1973). In this case D is the equivalent depth corresponding to either the external mode or to one of the internal modes. Our assumption is that for periods of a few days equation (2.1) is a reasonable model of large-scale atmospheric flow.

The dynamics of a numerical weather prediction model are also governed by an approximation of equation (2.1):

$$\frac{d}{dt}\left(a^{-2} \tilde{\nabla}^2 \tilde{\psi} - L^{-2} \tilde{\psi} + f\right) = \tilde{Q}. \qquad (2.2)$$

The tilde represents the numerical truncation effect in the operators $\tilde{d}/dt$ and $\tilde{\nabla}^2$ on the one hand, and the errors in the parameterization of the physical forcing, $\tilde{Q}$, on the other.

It follows that forecast errors $\delta\psi = \tilde{\psi} - \psi$ will also be governed to a good approximation by a conservation equation of potential vorticity, which does not contain the planetary vorticity term f:

$$\frac{d}{dt}\left(a^{-2}\nabla^2\delta\psi - L^{-2}\delta\psi\right) = \text{errors}; \qquad (2.3)$$

we let the errors in the right-hand side of (2.3) represent all the approximations, physical and numerical, made in equation (2.1) and, a fortiori, in equation (2.2). At the initial time, t=0, ψ is obtained from observations of the atmospheric state ψ which are also made with certain errors:

$$\delta\psi = \text{errors} \quad \text{at } t=0. \qquad (2.4)$$

If the errors in both Eq. (2.3) and the initial conditions (2.4) were zero, then one would obtain that the potential vorticity of the error will remain identically zero

$$(a^{-2}\nabla^2 - L^{-2})\,\delta\psi = 0$$

at all times $t > 0$.

In the presence of purely random errors, we can combine Eqs. (2.3) and (2.4) to yield a time-independent equation governing forecast errors. This equation is a stochastically forced steady-state potential vorticity equation on an f-plane:

$$(a^{-2}\nabla^2 - L^{-2})\,\delta\psi = F_t(0, \lambda; \omega). \qquad (2.5)$$

We take F_t to be random white noise, corresponding to different realizations of atmospheric processes labeled by ω, at time

$t>0$. We expect Eq. (2.5) to be a good representation of the structure of the forecast error field whenever systematic errors in Eq. (2.1) and (2.2) are small. It will cease to be valid at time scales longer than a day or two, because the errors in the approximation of the nonlinear terms, $\tilde{d}/dt-d/dt$, as well as in the parameterization of physical processes, $\tilde{Q}-Q$, become sizeable and nonrandom. We may also expect that Eq. (2.5) will be less accurate in the Northern Hemisphere than in the Southern Hemisphere, because topographic forcing and land-sea contrast are more important in the former than in the latter.

The statistical properties of F_t, in particular its variance σ_t^2, might change with time. Since t in (2.5) is only a parameter, we shall consider a fixed σ^2 in the sequel. The value of σ affects only the amplitude, and not the structure of the solution.

The Rossby radius of deformation L depends on the equivalent depth D and on the sine of latitude:

$$L^{-2}= (4\ \Omega^2/gD)\ \sin^2\theta. \qquad (2.6)$$

For simplicity, we assume that one vertical model dominates the error field, and shall determine the value of the equivalent depth that best fits the data.

Summarizing, we will study the equation for the <u>geopotential error field</u> ϕ,

$$(\nabla^2 - c_o \sin^2\theta\ )\ \phi = F(\lambda,\theta;\omega), \qquad (2.7)$$

where Eq. (2.5) was multiplied by the constant $f_o a^2$, and F is a spatially multi-dimensional noise process:

$$E\{F(\xi;\ \omega)\}=0, \qquad (2.8a)$$

$$E\{F(\xi_1;\omega)\ F\ (\xi_2;\omega)\} = \sigma^2\delta\ (\xi_1-\xi_2). \qquad (2.8b)$$

Here E is the expectation operator or ensemble average over the individual realization ω, $\xi=(\theta,\lambda)$ is the position vector, and σ^2 a prescribed variance.

We are mainly interested in the covariance function.

$$\Gamma(\xi_1,\xi_2) = E\ \{\phi(\xi_1;\omega)\ \phi\ (\xi_2;\omega)\} \qquad (2.9)$$

of the solution $\phi\ (\xi;\omega)$. The reason for our interest in Γ is that interpolation formulae for assimilation of atmospheric data require Γ as the basic statistical information.

In the following four sections, our methods for the solution of (2.7) and for the computation of (2.9) are described and compared.

3. Series solution of the model equation

Consider an expansion of ϕ ,

$$\phi(\theta,\lambda) = \sum_{n=0}^{\infty} \sum_{m=-n}^{n} B_n^m Y_n^m , \qquad (3.1)$$

in the spherical harmonics Y_n^m ,

$$Y_n^m(\theta,\lambda) = e^{im\lambda} P_n^m(\sin\theta) = e^{im\lambda} p_n^m(\mu) . \qquad (3.2a)$$

Here $\mu = \sin\theta$ and $P_n^m(\mu)$ are the associated Legendre functions (Courant and Hilbert, 1953; Hobson, 1955),

$$p_n^m(\mu) = \frac{(1-\mu^2)^{m/2}}{2^n n!} \frac{d^{n+m}}{d\mu^{n+m}} (\mu^2-1)^n , \qquad (3.2b)$$

normalized so that

$$\int_0^{2\pi} \int_{-1}^{1} Y_n^m \left(Y_{n'}^{m'}\right)^* d\mu \, d\lambda = 4\pi \frac{(2n+1)(n-m)!}{(n+m)!} \delta_{m,m'} \delta_{n,n'}$$

$$\equiv A_n^m \delta_{m,m'} \delta_{n,n'} ; \qquad (3.3)$$

$( )^*$ denotes complex conjugation.

The representation (3.1) would diagonalize Eq. (2.2), provided the operator in (2.2) were a pure Helmholtz operator, i.e., only a constant, θ-independent term were added to the Laplacian ∇^2 . As it is, we shall show that (3.1) leads to a five-diagonal representation of (2.2).

The orthogonal functions $P_n^m(\mu)$ satisfy the three-term recursion relation

$$\mu P_n^s = \frac{n+s}{2n+1} P_{n-1}^s + \frac{n-s+1}{2n+1} P_{n+1}^s , \quad \text{for } n > 0 .$$

It follows that, for $n > 1$,

$$\mu^2 P_n^s = \tilde{\alpha}_{n-2}^s P_{n-2}^s + \tilde{\beta}_n^s P_n^s + \tilde{\gamma}_{n+2}^s P_{n+2}^s , \tag{3.4a}$$

where

$$\tilde{\alpha}_{n-2}^s = \left(\frac{n+s}{2n+1}\right)\left(\frac{n+s-1}{2n-1}\right), \tag{3.4b}$$

$$\tilde{\beta}_n^s = \left(\frac{n+s}{2n+1}\right)\left(\frac{n-s}{2n-1}\right) + \left(\frac{n-s+1}{2n+1}\right)\left(\frac{n+s+1}{2n+3}\right) , \tag{3.4c}$$

and

$$\tilde{\gamma}_{n+2}^s = \left(\frac{n-s+1}{2n+1}\right)\left(\frac{n-s+2}{2n+3}\right) . \tag{3.4d}$$

Note that $\tilde{\alpha}_q^{-q-2} = \tilde{\alpha}_q^{-q-1} = \tilde{\gamma}_q^q = \tilde{\gamma}_q^{q-1} = 0$ for $q \geq 0$.

Substituting the series (3.1), truncated at n=N, into Eq. (2.2) we have

$$(\nabla^2 - c_0 \sin^2\theta)\phi^{(N)} \equiv$$

$$(\nabla^2 - c_0 \sin^2\theta) \sum_{n=0}^{N} \sum_{m=-n}^{n} B_n^m Y_n^m \equiv$$

$$(\nabla^2 - c_0\mu^2)\left[B_0^0 Y_0^0 + B_1^{-1} Y_1^{-1} + B_1^0 Y_1^0 + B_1^1 Y_1^1 + \sum_{n=2}^{N} \sum_{m=-n}^{n} B_n^m Y_n^m \right] = F. \tag{3.5}$$

On the unit sphere,

$$\nabla^2 Y_n^m = - n(n+1) Y_n^m \ . \tag{3.6}$$

The first few terms of the five-term recursion (3.4) are given by

$$\mu^2 Y_0^0 = \mu^2 P_0^0 = \mu^2 = \frac{2}{3}\left[\frac{1}{2}(3\mu^2-1)\right] + \frac{1}{3} = \frac{2}{3} P_2^0 + \frac{1}{3} P_0^0 = \frac{2}{3} Y_2^0 + \frac{1}{3} Y_0^0 \ ,$$

$$\mu^2 Y_1^0 = \mu^2 P_1^0 = \mu^3 = \frac{2}{5}\left[\frac{1}{2}(5\mu^3-3\mu)\right] + \frac{3}{5}\mu = \frac{2}{5} P_3^0 + \frac{3}{5} P_1^0 = \frac{2}{5} Y_3^0 + \frac{3}{5} Y_1^0 \ ,$$

$$\mu^2 Y_1^{-1} = e^{-i\lambda}\mu^2 P_1^{-1} = e^{-i\lambda}\mu P_2^{-1} = e^{-i\lambda}\left[\frac{1}{5} P_1^{-1} + \frac{4}{5} P_3^{-1}\right] = \frac{1}{5} Y_1^{-1} + \frac{4}{5} Y_3^{-1} \ ,$$

and

$$\mu^2 Y_1^1 = e^{i\lambda}\mu^2 P_1^1 = e^{i\lambda}\mu\left[\frac{1}{3} P_2^1\right] = \frac{1}{3} e^{i\lambda}\left[\frac{3}{5} P_1^1 + \frac{2}{5} P_3^1\right] = \frac{3}{15} Y_1^1 + \frac{2}{15} Y_3^1 \ .$$

Thus (3.5) can be rewritten as

$$B_0^0\left[-c_0\left(\frac{2}{3} Y_2^0 + \frac{1}{3} Y_0^0\right)\right] + B_1^{-1}\left[-2 Y_1^{-1} - c_0\left(\frac{1}{5} Y_1^{-1} + \frac{4}{5} Y_3^{-1}\right)\right]$$

$$+ B_1^0\left[-2 Y_1^0 - c_0\left(\frac{2}{5} Y_3^0 + \frac{3}{5} Y_1^0\right)\right] + B_1^1\left[-2 Y_1^1 - c_0\left(\frac{3}{15} Y_1^1 + \frac{2}{15} Y_3^1\right)\right]$$

$$+ \sum_{n=2}^{N} \sum_{m=-n}^{n} B_n^m \left\{\left[-c_0 \tilde{\alpha}_{n-2}^m\right] Y_{n-2}^m + \left[-n(n+1) - c_0 \tilde{\beta}_n^m\right] Y_n^m + \right.$$

$$\left. + \left[-c_0 \tilde{\gamma}_{n+2}^m\right] Y_{n+2}^m \right\} = F \ . \tag{3.7}$$

Define

$$\beta_n^m = \left[-n(n+1) - c_0\ \tilde{\beta}_n^m\right] A_n^m \ , \tag{3.8a}$$

$$\alpha_{n-2}^m = \left[- c_0\ \tilde{\alpha}_{n-2}^m\right] A_{n-2}^m \ , \tag{3.8b}$$

and

$$\gamma_{n+2}^m = \left[- c_0\ \tilde{\gamma}_{n+2}^m\right] A_{n+2}^m \ . \tag{3.8c}$$

Multiplying both sides of Eq.(3.7) by $(Y_k^j)^*$ and integrating, we have

$$\int_0^{2\pi} d\lambda \int_{-1}^{1} (Y_k^j)^* \{\text{LHS}\}\ d\mu = \int_0^{2\pi} d\lambda \int_{-1}^{1} (Y_k^j)^* F(\mu,\lambda)\ d\mu. \tag{3.9}$$

We denote the spherical harmonic coefficients of F, given by the integral on the right hand side, by F_k^j . Given F_k^j , we wish to solve for the coefficients B_n^m of ϕ . We have

$$C_1\ B_0^0 + \alpha_0^0\ B_2^0 = F_0^0 \ , \ C_1 = -c_0\ A_0^0/3 \ ,$$

$$C_2\ B_1^0 + \alpha_1^0\ B_3^0 = F_1^0 \ , \ C_2 = -(2+\tfrac{3}{5}\ c_0) A_1^0 \ ,$$

$$\beta_2^0\ B_2^0 + \alpha_2^0\ B_4^0 + C_3\ B_0^0 = F_2^0 \ , \ C_3 = \tfrac{-2}{3}\ c_0\ A_2^0 \ ,$$

$$\beta_3^0\ B_3^0 + \alpha_3^0\ B_5^0 + C_4\ B_1^0 = F_3^0 \ , \ C_4 = -\ \tfrac{2}{5}\ c_0\ A_3^0 \ ,$$

$$\beta_k^0\ B_k^0 + \alpha_k^0\ B_{k+2}^0 + \gamma_k^0\ B_{k-2}^0 = F_k^0 \ , \ 4 \leq k \leq N-2 \ ,$$

$$\beta^0_{N-1}\, B^0_{N-1} + \gamma^0_{N-1}\, B^0_{N-3} = F^0_{N-1} \ ,$$

$$\beta^0_N \ B^0_N + \gamma^0_N\, B^0_{N-2} = F^0_N \ .$$

The $N+1$ equations for F^0_k, $0 \le k \le N+1$, can be put into matrix vector form as a five-diagonal system in B^0_n, $0 \le n \le N+1$:

$$\left\{ \begin{bmatrix} \beta^0_2 & 0 & \alpha^0_2 & 0 & \cdots & 0 \\ 0 & \beta^0_3 & 0 & \alpha^0_3 & & \\ \gamma^0_4 & 0 & & & & 0 \\ & & & & & \alpha^0_{N-2} \\ 0 & & & & & 0 \\ & & & & & \\ 0 & \cdots & 0 & \gamma^0_N & 0 & \beta^0_N \end{bmatrix} + \begin{bmatrix} D_1 & 0 & \cdots & 0 \\ 0 & D_2 & 0 & \cdots \\ & & & \\ 0 & & & 0 \\ & & & \\ 0 & \cdots & & 0 \end{bmatrix} \right\} \begin{bmatrix} B^0_2 \\ B^0_3 \\ \vdots \\ \\ B^0_N \end{bmatrix} = \begin{bmatrix} F^0_2 - \dfrac{F^0_0\, C_3}{C_1} \\ F^0_3 - \dfrac{F^0_1\, C_4}{C_2} \\ F^0_4 \\ \vdots \\ F^0_N \end{bmatrix} \ , \tag{3.10.0}$$

where

$$D_1 = -C_3\, \alpha^0_0 / C_1 \qquad D_2 = -C_4\, \alpha^0_1 / C_2 \ .$$

The equations for F^1_k are

$$C_6\, B^1_1 + \alpha^1_1\, B^1_3 = F^1_1 \ , \quad C_6 = -\left(2 + \frac{3}{15} c_0\right) A^1_1 \ ,$$

$$\beta^1_2\, B^1_2 + \alpha^1_2\, B^1_4 = F^1_2 \ ,$$

$$\beta^1_3\, B^1_3 + \alpha^1_3\, B^1_5 + C_7\, B^1_1 = F^1_3, \quad C_7 = -\frac{2}{15}\, c_0\, A^1_3 \ ,$$

$$\beta_k^1 B_k^1 + \alpha_k^1 B_{k+2}^1 + \gamma_k^1 B_{k-2}^1 = F_k^1, \quad 4 \leq k \leq N-2 ,$$

$$\beta_{N-1}^1 B_{N-1}^1 + \gamma_{N-1}^1 B_{N-3}^1 = F_{N-1}^1 ,$$

$$\beta_N^1 B_N^1 + \gamma_N^1 B_{N-2}^1 = F_N^1 .$$

They have the five-diagonal form,

$$\left\{ \begin{bmatrix} \beta_2^1 & 0 & \alpha_2^1 & 0 & 0 \\ 0 & & & & \\ \gamma_4^1 & & & & \alpha_{N-2}^1 \\ 0 & & & & 0 \\ 0 & 0 & \gamma_N^1 & 0 & \beta_N^1 \end{bmatrix} + \begin{bmatrix} 0 & 0 & 0 & 0 \\ 0 & D_3 & 0 & \\ 0 & 0 & 0 & 0 \\ 0 & 0 & & 0 \end{bmatrix} \right\} \begin{bmatrix} B_2^1 \\ B_3^1 \\ \vdots \\ B_N^1 \end{bmatrix} = \begin{bmatrix} F_2^1 \\ F_3^1 - \dfrac{C_7 F_1^1}{C_6} \\ F_4^1 \\ \vdots \\ F_N^1 \end{bmatrix} \tag{3.10.1}$$

where $D_3 = - \alpha_1^1 . C_7 / C_6$.

We have a similar system for F_k^{-1} :

$$C_8\, B_1^{-1} + \alpha_1^{-1}\, B_3^{-1} = F_1^{-1}, \text{ where } C_8 = (-2 - c_0\, \tfrac{1}{5})\, A_1^{-1} ,$$

$$\beta_1^{-1}\, B_2^{-1} + \alpha_2^{-1}\, B_4^{-1} = F_2^{-1} ,$$

$$\beta_3^{-1}\, B_3^{-1} + \alpha_3^{-1}\, B_5^{-1} + C_9\, B_1^{-1} = F_3^{-1}, \text{ where } C_9 = (-c_0\, \tfrac{4}{5})\, A_3^{-1},$$

$$\beta_k^{-1}\, B_k^{-1} + \alpha_k^{-1}\, B_{k+2}^{-1} + \gamma_k^{-1}\, B_{k-2}^{-1} = F_k^{-1}, \quad 4 \le k \le N-2 ,$$

$$\beta_{N-1}^{-1}\, B_{N-1}^{-1} + \gamma_{N-1}^{-1}\, B_{N-3}^{-1} = F_{N-1}^{-1} ,$$

$$\beta_N^{-1}\, B_N^{-1} + \gamma_N^{-1}\, B_{N-2}^{-1} = F_N^{-1} .$$

All the other systems are of the form

$$\begin{pmatrix} \beta_k^{\pm k} & 0 & \alpha_k^{\pm k} & 0 & \cdots & 0 \\ 0 & \beta_{k+1}^{\pm k} & & \ddots & \ddots & 0 \\ \gamma_{k+2}^{\pm k} & & \ddots & \ddots & \alpha_{N-2}^{\pm k} & \\ 0 & \ddots & \ddots & \ddots & 0 & \\ \vdots & \ddots & \ddots & & & \\ 0 & \cdots & 0 & \gamma_N^{\pm k} & 0 & \beta_N^{\pm k} \end{pmatrix} \begin{pmatrix} B_k^{\pm k} \\ B_{k+1}^{\pm k} \\ \cdot \\ \cdot \\ \cdot \\ B_N^{\pm k} \end{pmatrix} = \begin{pmatrix} F_k^{\pm k} \\ F_{k+1}^{\pm k} \\ \cdot \\ \cdot \\ \cdot \\ F_N^{\pm k} \end{pmatrix} ,$$

$$k=2, \ldots, N , \qquad (3.10.k)$$

In (3.10.k)

$$\beta_k^j B_k^j + \alpha_k^j B_{k+2}^j = F_k^j$$

$$\text{for} \begin{cases} |j| = 2,3,\ldots, N-3 \quad \text{and} \quad k = j, j+1 \ ; \\ |j| = N-2 \quad \text{and} \quad k = N-2 \ , \end{cases}$$

$$\beta_k^j B_k^j + \alpha_k^j B_{k+2}^j + \gamma_k^j B_{k-2}^j = F_k^j$$

$$\text{for} \quad |j| = 2,3,\ldots, N-4 \quad \text{and} \quad k = j+2,\ldots, N-6 \ ;$$

$$\beta_k^j B_k^j = F_k^j$$

$$\text{for} \begin{cases} |j| = N-2 & \text{and} \quad k = N-1 \ , \\ |j| = N-1 & \text{and} \quad k = N-1, N \ , \\ |j| = N & \text{and} \quad k = N \ ; \end{cases}$$

$$\beta_k^j B_k^j + \gamma_k^j B_{k-2}^j = F_k^j$$

$$\text{for} \begin{cases} |j| = 2,3,\ldots, N-3 \quad \text{and} \quad k = N, N-1 \ , \\ |j| = N-2 \quad \text{and} \quad k = N \ . \end{cases}$$

Each of the above linear systems are penta diagonal. They can be solved by the LU factorization algorithm given in Appendix A.

After solving for the B_n^m we wish to obtain the covariance function $\Gamma(\theta_1, \lambda_1; \theta_2, \lambda_2)$. More specifically, we are interested in the zonal covariances,

$$R(\theta, \lambda) = \Gamma(\theta, \lambda_0; \theta, \lambda_0 + \lambda) \ ; \qquad (3.11)$$

clearly $R(\theta,\lambda)$ is independent of λ_0. The zonal variances, $R_N(\theta,\lambda)$, corresponding to a truncated solution $\phi^{(N)}$, are given by

$$
\begin{aligned}
R_N(\theta,\lambda) &= \int_0^{2\pi} \phi^{(N)}(\theta,y)\,\phi^{(N)}(\theta,y+\lambda)\,dy \\
&= \sum_{n=0}^{N} \sum_{n'=0}^{N} \sum_{m=-n}^{n} \sum_{m'=-n'}^{n'} B_n^m B_{n'}^{m'} P_n^m(\mu) P_{n'}^{m'}(\mu) \\
&\quad \cdot \int_0^{2\pi} e^{i[(m+m')y + m'\lambda]}\,dy \\
&= 2\pi \sum_{n=0}^{N} \sum_{n'=0}^{N} \sum_{m=-n}^{n} B_n^m B_{n'}^{-m} P_n^m(\mu) P_{n'}^{-m}(\mu)\, e^{-im\lambda} \\
&= 2\pi \left\{ \sum_{n=0}^{N} \left[(B_n^0 P_n^0)^2 + 2 B_n^0 P_n^0 \sum_{n'=n+1}^{N} B_{n'}^0 P_{n'}^0 \right] \right. \\
&\quad \left. + 2 \sum_{n=1}^{N} \sum_{n'=1}^{N} \sum_{m=1}^{n} B_n^m B_{n'}^{-m} P_n^m P_{n'}^{-m} \cos(m\lambda) \right\}.
\end{aligned}
\tag{3.12}
$$

Clearly, (3.12) does not provide a computationally efficient way of obtaining $R_N(\theta,\lambda)$ for large N .

In the following two sections we shall use the numerical approach of directly inverting (2.2) for fixed RHS, ω = constant. $R(\theta,\lambda)$ will be computed by summing over correlation products of solutions for various ω . A fast solver for the inversion of (2.2) with given RHS(ω = const.) is presented next.

4. A generalized fast Poisson solver

A fast solver for the equation,

$$[\nabla^2 + C(\theta)]\phi = f(\theta,\lambda), \tag{4.1}$$

with $C(\theta)$ = constant, is available in the NCAR software library (Swarztrauber and Sweet, 1975). This program was modified and extended to solve Eq.(4.1). The NCAR version takes the finite-difference approximation to Eq.(4.1) as

$$\begin{aligned}
&\frac{1}{\Delta\theta^2 \sin\theta_i}\Big[\sin(\theta_i + \tfrac{1}{2}\Delta\theta)(\theta_{i+1,j} - \theta_{i,j}) \\
&\quad - \sin(\theta_i - \tfrac{1}{2}\Delta\theta)(\phi_{i,j} - \phi_{i-1,j})\Big] \\
&\quad + \frac{1}{(\Delta\lambda \sin\theta_i)^2}(\phi_{i,j+1} - 2\phi_{i,j} + \phi_{i,j-1}) + C\phi_{i,j} \\
&\quad = f(\theta_i, \lambda_j) ,
\end{aligned} \tag{4.2}$$

where C = const ,

$$\theta_i = (i-1)\Delta\theta \ , \ \lambda_j = (j-1)\Delta\lambda \ ,$$

$$\phi_{i,j} = \phi(\theta_i, \lambda_j) \ , \ \Delta\theta = \pi/M \ , \Delta\lambda = 2\pi/N \ ,$$

$$i = 1,2,\ldots,M+1 \ , \quad j = 1,2,\ldots,N+1 \ .$$

In the NCAR version, the option of solving (4.1) in a subdomain on the surface of the sphere exists. This option was removed in our version. Our extended program then takes C in eq. (4.2) to be $C_i = C(\theta_i)$. No futher modifications of the original program were required. The modified program was extensively tested (Table 1).

We conclude from the numerical tests that the modified version of the solver has the desirable properties of the original one: second-order accuracy with respect to discretization error, and machine accuracy in linear system solving for a moderate-size mesh (32x64).

5. Monte-Carlo solution of the model equation

We wish to solve Eq. (2.7) with the RHS $F(\theta,\lambda;\omega)$ being white noise. The solution is approximated by Monte-Carlo simulation. In other words, Eq.(4.1) is solved for an individual realization of the white noise process $F(\theta,\lambda;\omega)$, namely $f(\theta,\lambda)$. A large number N of samples $f_1, f_2, \ldots, f_n$ is drawn from the process $F(\theta,\lambda;\omega)$. Let $\phi_n(\theta,\lambda)$ be the solution of (4.1) with $f_n(\theta,\lambda)$ as RHS and let

$$\phi^{(N)}(\theta,\lambda) = \frac{1}{N} \sum_{n=1}^{N} \phi_n \, .$$

Our Monte-Carlo solution of (2.7) is $\phi^{(N)}$.

If $\{f_n, n=1,2,\ldots,N\}$ are simply independent samples of F, then a very large N is needed in order for $\phi^{(N)}$ to be a good approximation to the true solution ϕ of (2.2); i.e., $\phi^{(N)}$ has a large variance around its expected value ϕ, even for large N. In order to accelerate this convergence of $\phi^{(N)}$ to ϕ, we used a technique for variance reduction called stratified sampling (Appendix B).

Eq. (2.7) was discretized with 19 grid points in the meridional direction and 32 grid points in the longitudinal direction. The poles are grid points, and the equator is a grid line.

We obtained the zonal correlations from our simulation as follows. Let the normalized correlation r_κ of an individual realization $\phi_\kappa = \phi_\kappa(\theta,\lambda)$ be defined as

$$r_\kappa(\theta,\lambda) = \frac{\int_0^{2\pi} \phi_\kappa(\theta,\lambda')\phi_\kappa(\theta,\lambda'+\lambda)d\lambda'}{\int_0^{2\pi} \phi_\kappa^2(\theta,\lambda)d\lambda} \; ; \qquad (5.1a)$$

notice the slight change of notation from (3.11). $r_\kappa(\theta,\lambda)$ depends only on the separation in longitude, λ, between two points (θ,λ_0) and $(\theta,\lambda_0+\lambda)$ on a circle of latitude θ, and not on their position λ_0. This is due to the rotational invariance with respect to longitude of (2.2). Now the correlation function $r(\theta,\lambda)$ is approximately by

$$r^{(N)}(\theta,\lambda) = \frac{1}{N} \sum_{\kappa=1}^{N} r_\kappa \quad . \tag{5.1b}$$

Here we assume that the mean of ϕ_κ is zero. We took a large number N of correlation realizations, r_κ, and averaged them to obtain statistically stable results.

The integrals in (5.1a) were evaluated by the trapezoidal rule,

$$R_j = R_\kappa(\theta,j\Delta\lambda) = \sum_{k=0}^{M-1} \phi_k \, \phi_{k+j} \, \Delta\lambda, \tag{5.2}$$

where we have dropped the argument θ and the subscript κ, so that $\phi_k = \phi_\kappa(\theta,k\Delta\lambda)$.

The convolution product $\sum_{k=0}^{M-1} \phi_k\phi_{k+j}$ can be computed using Fast Fourier Transform ideas (Henrici, 1979). Let $\mathbb{R}$ be the reversion operator; for a periodic sequence $\{x_i\}$, it is defined as

$$(\mathbb{R}x)_m = x_{-m} \quad . \tag{5.3a}$$

Let $\mathbb{F}$ be the discrete Fourier operator defined for two sequences $\{x_i\}$ and $\{U_i\}$ of period M by $\mathbb{F}\vec{x} = \vec{U}$; component-wise

$$U_m = \frac{1}{M} \sum_{k=0}^{M-1} \omega^{-mk} \, x_k \quad , \tag{5.3b}$$

with $\omega = \exp(\frac{2\pi i}{M})$. It follows that the inverse Fourier operator is defined by $\mathbf{F}^{-1} = M\mathbf{F}\ \mathbf{R} = M\ \mathbf{R}\ \mathbf{F}$.

Consider the Hadamard product $\vec{x}\cdot\vec{y}$ of two sequences $\vec{x}$ and $\vec{y}$, $x \cdot y = \{x_k\ y_k\}$, and let

$$\vec{U} = \mathbf{F}\ \vec{x},\ \vec{V} = \mathbf{F}\ \vec{y}\ .$$

The Fourier transform of $\vec{x}\cdot\vec{y}$ is then

$$\begin{aligned}(\mathbf{F}\ (\vec{x}\cdot\vec{y}))_m &= \frac{1}{M}\sum_{k=0}^{M-1} x_k\ y_k\ \omega^{-km} \\ &= \frac{1}{M}\sum_{k=0}^{M-1} x_k \sum_{\ell=0}^{M-1} V_\ell\ \omega^{\ell k}\ \omega^{-km} \\ &= \sum_{\ell=0}^{M-1} V_\ell\ \frac{1}{M}\sum_{k=0}^{M-1} x_k \omega^{-(m-\ell)k} \\ &= \sum_{\ell=0}^{M-1} V_\ell\ U_{m-\ell}\ .\end{aligned}$$

For any two M-periodic sequences $\vec{U} = \{U_k\}$ and $\vec{V} = \{V_k\}$, we define the convolution product $\vec{C} = \{C_k\}$ by

$$C_m = \sum_{k=0}^{M-1} V_k\ U_{m-k} = \sum_{k=0}^{M-1} U_k\ V_{m-k}\ .$$

We denote this convolution product by $\vec{C} = \vec{U} * \vec{V}$.

Thus

$$\mathbf{F}\ (\vec{x}\cdot\vec{y}) = \mathbf{F}\ \vec{x} * \mathbf{F}\vec{y}\ . \qquad (5.4)$$

Taking into account that $\phi(\theta,\lambda)$ is 2π-periodic with respect to λ, we have that

$$R_j = \sum_{k=0}^{M-1} \phi_k \, \phi_{k+j} = \sum_{k=0}^{M-1} \phi_{k-j} \, \phi_k = \sum_{k=0}^{M-1} \phi_k \, \phi_{-(j-k)}$$

or

$$\vec{R} = \vec{\phi} * \vec{\phi}$$

$$= \mathbf{F} \left((\mathbf{F}^{-1}\vec{\phi}) \cdot (\mathbf{F}^{-1}\mathbf{R}\,\vec{\phi}) \right)$$

$$= M^2 \, \mathbf{F}\left((\mathbf{R}\,\mathbf{F}\vec{\phi}) \cdot (\mathbf{R}\,\mathbf{F}\,\mathbf{R}\,\vec{\phi}) \right)$$

$$= M^2 \, \mathbf{F}\,\mathbf{R} \left((\mathbf{R}\,\mathbf{F}\vec{\phi}) \cdot (\mathbf{F}\vec{\phi}) \right)$$

$$= M \, \mathbf{F}^{-1} \left((\mathbf{R}\,\mathbf{F}\vec{\phi}) \cdot (\mathbf{F}\vec{\phi}) \right)$$

$$= M \, \mathbf{F}^{-1} \left((\mathbf{F}\vec{\phi})^* \cdot (\mathbf{F}\vec{\phi}) \right) .$$

After calculating the correlations $r_j = r_\kappa(\theta, j\Delta\lambda)$ for each latitude θ at uniform angular distance intervals $\Delta\lambda$, we use spline interpolation to obtain the correlations $r_\kappa(\theta,s)$ in terms of spherical distance s around a circle of latitude, at regular intervals $\Delta s = 200$km.

Our experiments showed that Monte-Carlo simulation, even using variance reduction, converged very slowly. It required a large number of realizations. But the solution had the expected behavior, namely $R(\theta, s/a) \sim \exp(-s/s_0)$, where $s_0(\theta) \sim \sin\theta$, and a is the radius of the earth.

6. An equation for the covariance function

Given the linear equation with deterministic coefficients (2.7) for $\phi = \phi(\xi;\omega)$, it is easy to obtain a linear equation for the covariance function $\Gamma(\xi_1, \xi_2)$, defined in (2.3). Writing (2.7) symbolically as

$$L\phi = F(\xi;\omega) \tag{6.1a}$$

with

$$L = (\nabla^2 - c_0 \sin^2\theta) \ , \tag{6.1b}$$

we are interested in the ensemble average of $\phi(\xi_1;\omega)\phi(\xi_2;\omega)$.

Let L_1, L_2 be the operator L written with respect of the position vectors ξ_1 and ξ_2, respectively, $\phi_1 = \phi(\xi_1;\omega)$, $\phi_2 = \phi(\xi_2;\omega)$, and $F_{1,2} = F(\xi_{1,2};\omega)$. Then

$$\phi_2 \, L_1 \, \phi_1 = \phi_2 \, F_1 \ ;$$

applying L_2 and taking the ensemble average, we have

$$E \, L_2 \, \phi_2 \, L_1 \, \phi_1 = L_1 \, L_2 \, E \, \phi_1 \, \phi_2$$

$$= E \, L_2 \, \phi_2 \, F_1 = E \, F_1 \, F_2 = \sigma^2 \delta(\xi_1 - \xi_2) \ .$$

Here we used the fact that E, L_1, L_2 are all linear operators and commute with each other, since they operate on the independent variables ω, ξ_1 and ξ_2, respectively. We thus obtain for

$$\Gamma(\xi_1, \xi_2) = E\phi_1 \, \phi_2$$

the deterministic linear equation

$$L_1 L_2 \Gamma(\xi_1, \xi_2) = \sigma^2 \delta(\xi_1 - \xi_2) \ . \qquad (6.2)$$

A rigorous derivation of (6.2), under suitable assumptions on the operator L and data F, appears in Bécus and Cozzarelli (1976). We are only interested in computing

$$R(\theta,\lambda) = \Gamma(\theta,0;\theta,\lambda) \ . \qquad (6.3)$$

To solve (6.2) for $R(\theta,\lambda)$, we start by solving numerically

$$L_1 H(\xi_1; \xi_2) = \delta(\xi_1 - \xi_2) \qquad (6.4)$$

for each ξ_2. First, the solution $H(\xi_1; \xi_2)$ for given ξ_2 is obtained for $\lambda_2 = 0$. More precisely, for $\xi_2 = (k_2\Delta\theta, 0)$, $k_2 = 0,1,\ldots, K-1$, we compute $H(k_1\Delta\theta, j_1\Delta\lambda; \xi_2)$, $k_1 = 0,1,\ldots, K-1$, $j_1 = 0,1,\ldots, J-1$.

The solution $H(\xi_1;\xi_2)$ for all other $\xi_2 = (k_2\Delta\theta, j_2\Delta\lambda)$, $j_2 = 1,2,\ldots,J-1$, $k_2 = 0,1,\ldots,K-1$ is then obtained from the previously computed $H(\xi_1;\xi_2)$ by

$$H(k_1\Delta\theta, j_1\Delta\lambda; k_2\Delta\theta, j_2\Delta\lambda) = H(k_1\Delta\theta, (j_1-j_2)\Delta\lambda; k_2\Delta\theta, 0) \ . \qquad (6.5)$$

In other words, only K "inversions" of L_1 are needed, rather than KJ in solving (6.4), viz., $O(K^2J)$ operations rather than

$O(K^2J^2)$ have to be performed. Furthermore, (6.3) shows that we need only solve

$$L_2\Gamma(\xi_1;\ \xi_2) = H(\xi_1;\xi_2) \qquad (6.6)$$

for $H(\theta,0;\xi_2)$, since we are only interested in $R(\theta,\lambda)$, rather than in the full $\Gamma(\xi_1;\xi_2)$. Hence, only K "inversions" of L_2 are needed, leading to a total $O(K^2J)$ operation count to obtain $R(\theta,\lambda)$ from (6.2). In our numerical solution of (6.2) directly is much more efficient in order to compute $R(\theta,\lambda)$ than a Monte-Carlo solution of (2.7). First, N, the number of realizations necessary for a good approximation $\phi^{(N)}$ to ϕ is considerably larger than 2K. Second, here the covariances are obtained directly, without the need for computing convolution products of $\phi^{(N)}$; the later requires $O(KJ^2\log J)$ additional operations.

The numerical results we present in the next section depend only on the form of Eq. (2.7), not on the method used for obtaining it solution and the covariance of this solution. The results were obtained by the most efficient method, that described in the present section. Some of the results were futher confirmed by using Monte-Carlo simulation with variance reduction (Section 5 and Appendix B). The zonal covariances $R(\theta,\lambda)$ obtained by solving (6.2) were divided by the local variance to obtain zonal correlations $r(\theta,\lambda)$ as in (5.1).

7. Numerical results

The starting point of this study was the development and testing of a model which will reproduce the latitude dependence of zonal correlations of $T^o - T^f$ observed in GHA. The model is governed by Eqs. (2.7) and (6.2).

a. Data sets

The model was tested first using the data on which Figs. 2a-d of GHA were based, namely vertically averaged correlations of the difference field, $T^o - T^f$, between satellite-derived and model forecast temperatures. This test was based on the hydrostatic connection between temperature and layer thickness, which should make ϕ and vertically averaged T interchangeable at the level of approximation of our model. Model correlations exhibited the same tightening with increasing latitude as that of the data, for any reasonable value of the parameter c_o.

After this preliminary test, we proceeded to study if our model results would fit observed 500mb geopotential height data. We considered first NMC analyses of 500mb heights for the DST-6 period, January-March 1976, and for January 1978, available on tape at GLAS. Zonal correlations for the analyzed fields every 12h over these periods were computed at different latitudes and averaged over time. The averaged correlation curves showed the typical damped cosine (Gandin, 1963; Thiébaux, 1977) or Bessel function behavior (J_0: Rutherford, 1972) of atmospheric fields. In particular, the curves crossed the s-axis, becoming negative at some distance $s_1 = s_1(\theta)$ which decreased with latitude. It is clear that our model will

not simulate such behavior: the covariance function $\Gamma(\xi_1, \xi_2)$ given by (6.2) cannot become negative. Indeed, the operator (-L) in Eq. (6.1) is monotone, i.e., $-L\,\phi \geq 0$ implies $\phi \geq 0$; this property is closely related to L satisfying a maximum principle. Thus $\delta(\xi_1-\xi_2) \geq 0$ implies $-L_2\Gamma(\xi_1,\xi_2) \geq 0$ and hence $\Gamma(\xi_1,\xi_2) \geq 0$, i.e., Γ is nonnegative for all values of ξ_1 and ξ_2. More rigorous proofs, not involving δ - functions, can be given, using the fact that $\Gamma(\xi_1,\xi_2)$ is closely related to the Green's function of the monotone operator $L_1\ L_2$.

The physical reason that correlations of observed geopotential data become negative at distances larger than s_1 is the presence of the planetary vorticity in the potential vorticity Eq. (2.1). The planetary vorticity varies with latitude and it is the $v\partial f/\partial\theta$ term that gives rise to Rossby waves, which have a characteristic horizontal wavelength of the order of several thousand kilometers. These waves dominate large-scale, mid-latitude flow and hence the statistical structure of mass fields at these latitudes. The variable planetary vorticity, however, is not present in the geopotential error equations (2.3) or (2.5). This makes it physically plausible that the horizontal error correlation should never become negative in our model.

Based on the evidence of the correlations for the difference fields $T^o - T^f$, we turned our attention to the model forecast fields of 500mb heights. One of the assimilation experiments performed at GLAS with DST-6 data, namely the one which, in

addition to conventional data, assimilated temperature data from two satellites by a time-continuous statistical method (experiment S2a, cf. GHA, Table 1) was used. Three-day forecasts had been performed from initial states produced by the assimilation cycle every 48h from 0000GMT 1 February 1976 till 0000GMT 4 March 1976. Table 2 shows the availability of forecast fields at synoptic epochs for all the forecasts, at the time our computations were carried out.

b. Model validation

We computed correlations for the difference fields $\phi^0 - \phi^f$, using NMC analyses as ϕ^0 and our experimental forecast fields as ϕ^f, for 12h 24h, 36h, and 48h forecasts (Table 3). These correlations were then compared with our model correlations, using different values of the nondimensional parameter c_o. As in the case of the temperature difference fields, model results and data were in good agreement for a certain range of values of c_o. The result which is apparently best for all error measures is boxed. This value seems to increase slightly with forecasting interval: it is 110 for 12h, 150 for 24h, 170 for 36h and 190 for 48h. For the combined 24h and 36h data set, it lies between 160 and 170.

c. Effects of vertical stratification

The stochastic model (2.7) gives good qualitative agreement with zonal correlations of experimental forecast errors, provided we use values of the constant c_o between 100 and 200. From Section 2,

$$c_o = 4\ \Omega^2 a^2/gD. \qquad (7.1)$$

For the external mode of the atmosphere, D ~ 10 km, this expression takes a value of $c_o \cong 10$. The lack of agreement with our results indicates that external, barotropic motions do not dominate the error field growth.

As a first step in accounting for the effect of vertical variations, we can use in (7.1) a reduced value of gravity, $g'=Sg$, that takes into account the stable stratification S,

$$S=(D/\theta_S)\, d\theta_S/dz,$$

of a standard atmosphere with potential temperature $\theta_S = \theta_S(z)$ (Pedlosky, 1979, Sec. 6.5). A typical value of the stratification parameter is S=0.1, which corresponds to a Brunt-Vaisala frequency of $N \cong 10^{-2}$ sec^{-1}, where $N^2=(g/\theta_S)d\theta_S/dz$.

Redefining c_o as:

$$c_o = 4\Omega^2 a^2/g'D, \qquad (7.2)$$

and substituting a value of g' based on S=0.1, we obtain $c_o \cong 100$. This is in much better agreement with our results.

A rigorous analysis of stratification effects would require a full three-dimensional separation of variables. Such a development does not seem to be warranted by the poor accuracy of the data. Stratification of the data by height would also impose serious restrictions on their statistical reliability, due to limited sample size.

We can interpret our results as indicating that forecast error growth is dominated by baroclinic motions in the atmosphere. Baroclinic instability is the most important dynamical instability in the extratropical atmosphere. Hence this aspect of our results is not entirely unexpected.

8. Discussion and conclusions

We have derived a stochastic-dynamic model for the global structure of the atmospheric mass field forecast error. The model is governed by a stochastically perturbed Helmholtz-type equation (2.7). The covariance function of the model's solutions has been shown to be governed by Eq. (6.2). The study originated in the observation (GHA) that zonal correlations of mass fields exhibit a strong latitude dependence, with radii of equal correlation becoming smaller at higher latitudes. An analysis of the potential vorticity equation, both for the atmosphere and for numerical weather prediction models, led to the derivation of our stochastic-dynamic model for the error field. The model supports the heuristic interpretation of the tightening of the correlations with latitude given in GHA, namely that the typical correlation radii vary with latitude in the same sense as the Rossby radius of deformation.

The observation (GHA) that correlation fields did not exhibit a strong vertical dependence led us to choose a single model parameter to represent the vertical structure. The value of this parameter, c_o, was determined so as to give the best quantitative fit between the second-order statistics of the model and of the data. The empirically determined value is consistent with baroclinic motion dominating the error growth field. The barotropic mode does not seem to play a major role.

The model results are in good agreement with actual numerical weather prediction errors, both for temperature and geopo-

tential fields. The differences between model and data are typically smaller than those between the data of one hemisphere and those of the other. We intend therefore to use the global correlation functions produced by the present model in the development of the GLAS statistical assimilation method. This should eliminate the inconsistency produced at present by the use of ad-hoc, meridionally stratified, empirical correlation functions (GHA).

The agreement between our stochastic model and actual forecast errors fields for 12 to 36 hour periods validates the assumptions on which the model was derived. Within this period, the difference between the potential vorticity fields of the atmosphere and of the numerical model forecast used in the comparison is well represented by white noise.

For periods shorter than 12 hours, the lack of balance in the initial data generates fast inertia-gravity waves in the model, which violate the quasi-geostrophic assumption implied in the potential vorticity equation. The use of a strongly damping time scheme, the Euler-backward scheme, in the GLAS second-order model makes these waves negligible after 12 hours. The use of an effective initialization scheme could eliminate this restriction.

For periods longer than 36 hours, the forecast errors become so large that the model equation (2.2) ceases to be a good representation of the atmospheric governing equation (2.1). The length of this limiting period is obviously model dependent. The forecast model used in obtaining our forecast error data,

the GLAS 9-level 4° latitude by 5° longitude, second order model, has rather large truncation errors. With higher resolution or higher accuracy models (e.g. Kalnay-Rivas and Hoitsma, 1979) we may expect that the stochastic model will remain valid for longer periods.

The observation that our stochastic model based on white-noise forcing fits Southern Hemisphere errors better than those of the Northern Hemisphere is also an interesting result. It indicates the validity of an increasingly well accepted point: that the lack of proper parameterization of the planetary-scale forcing can have a very important effect on the forecast errors.

The interplay between atmospheric statistics and dynamics which is stressed by this work points the way to further studies along similar lines. Allowing for such interplay in modeling efforts might help to improve our knowledge of both deterministic and stochastic aspects of atmospheric behavior.

A concrete step along this road would be to investigate the stochastically perturbed potential vorticity equation (2.1) itself, rather than its steady-state form (2.2). This would be a nonlinear, time-dependent Langevin-type equation for large-scale atmospheric flows. Its study appears considerably more difficult than that of the present model, but still accessible by Monte-Carlo simulation with variance reduction. We hope to report on such a study in a future publication.

Appendix A. Algorithm for penta-diagonal system

We solve

$$Ax = b \tag{A.1}$$

where A is penta-diagonal, by LU factorization

$$A = LU \ .$$

The factorization can be derived from the well-known one for tri-diagonal systems, by noticing that actually odd and even variables in (A.1) decouple. Hence

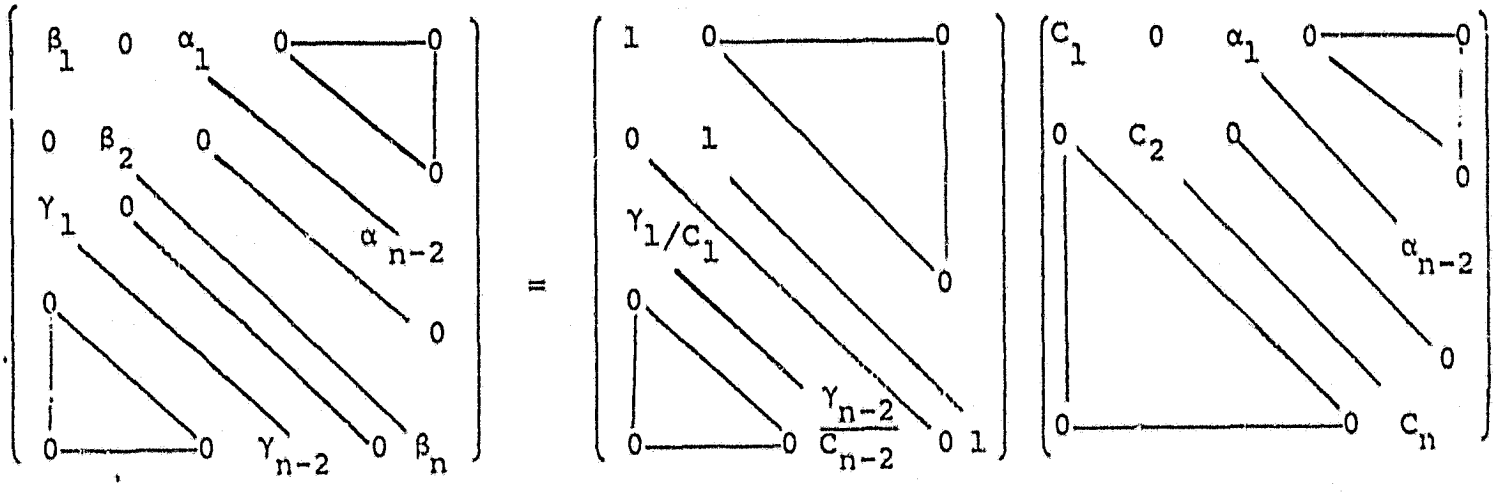

The algorithm can be performed in the following three steps.

Step 1: $C_1 = \beta_1$, $C_2 = \beta_2$,

$$C_k = \beta_k - (\gamma_{k-2}/C_{k-2})\alpha_{k-2} \ , \ k = 3,\ldots,n \ .$$

Step 2 (Forward elimination, i.e., solve $Ly = b$):

$$y_1 = b_1 \ , \ y_2 = b \ ,$$

$$y_k = b_k - \gamma_{k-2}\, y_{k-2}/c_{k-2} \ , \ k = 3,\ldots,n \ .$$

Step 3 (Back substitution, i.e., solve $Ux = y$):

$$x_n = y_n/c_n \ , \ x_{n-1} = y_{n-1}/c_{n-1} \ ,$$

$$x_k = (y_k - \alpha_k\, x_{k+2})/c_k \ , \ k = n-2,n-3,\ldots,1 \ .$$

Appendix B. Stratified sampling

Monte-Carlo simulation is a method for the solution of stochastic model equations using sample realizations. The individual realizations are computed by using pseudo-random number generators to specify the random functions prescribed as data of the equation. Basic random number generators produce variables which are to a good approximation uniformly distributed on the interval [-1,1] and stochastically independent.

We used the following stratified sampling procedure (Kleijnen, 1974, Ch.3). Let N be the number of realizations in our sample. We classify the random value taken by any sampled RHS, $f_i(\theta,\lambda)$, at each grid point (θ_j,λ_k) into exactly one of N classes. These classes are formed by dividing the range [-1,1] into N non-overlapping exhaustive intervals. We picked the range of each class to be of equal length. The functions $f_j(\theta,\lambda)$ and $f_k(\theta,\lambda)$ are made dependent for $j \neq k$, $j, k \in \{1,2,\ldots, N\}$, by taking at each grid point $f_j(\theta,\lambda)$ and $f_k(\theta,\lambda)$ from different classes. The objective of stratification is to lead to variance reduction.

We solve Eq. (4.1) with $f(\theta,\lambda) = f_i(\theta,\lambda)$ to obtain ϕ_i, $i = 1,2,\ldots, N$. Thus the ϕ_i themselves will be dependent. After experiments with both independent and stratified sampling, the superiority of the latter was clearly established. A sample size of N = 200 gave satisfactory results when using stratified sampling; independent sampling with N = 700 gave results whose variance was still much too large to be satisfactory.

Acknowledgement.

One of the authors (M.G.) was introduced to the study of inhomogeneous, anisotropic random fields by H. Jean Thiebaux and by Grace Wahba. Their published work (e.g., Thiebaux, 1977; Wahba, 1979) on modeling such random fields by stochastic differential equations, and conversations with them have been seminal to this model. George Papanicolaou has been most helpful in discussions about elliptic partial differential equations with fluctuations. Malvin Kalos has introduced us to Monte-Carlo simulation and variance reduction. Cecil E. Leith gave us the benefit of discussions and encouragement. J. Shukla offered useful comments on the statistical structure of atmospheric geopotential fields. Herbert Carus and Diego Edelmann provided the data sets in an easily readable form.

This work was supported by NASA Grants NSG-5034 (R.B.) and NSG-5130 (M.G.). Computations were carried out on the CDC 6600 of the Courant Mathematics and Computing Laboratory, New York University, under Contract EY-76-C-02-3077 with the U.S. Department of Energy. The typing was cheerfully performed by Julie Gonzalez and Karen DeHenzel. The manuscript was expertly edited by Carolyn Fonner.

References

Becus, G. A., and F. A. Cozzarelli, 1976a: The random steady state diffusion problem. I: Random generalized solutions to Laplaces equation, SIAM J. Appl. Math., 31, pp 134-147.

_____, 1976b: The random steady state diffusion problem. II: Random solutions to nonlinear, inhomogeneous, steady state diffusion problems SIAM J. Appl. Math., 31, pp 148-158.

_____, 1976c: The random steady-state diffusion problem, III: Solutions to random diffusion problems by the method of random successive approximations, SIAM J. Appl. Math., 31, pp 159-178.

Bengtsson, L., 1975: Four-dimensional data assimilation of meteorological observations, GARP Publ. Ser., 15, WMO/ICSU, Geneva, Switzerland 76 pp.

Charney, J. G., 1973: Planetary fluid dynamics, in Dynamic Meteorology, P. Morel (ed.), D. Reidel Publ. Co., Dordrecht-Holland/Boston-U.S.A., pp. 97-351.

Courant, R. and D. Hilbert, 1953: Methods of Mathematical Physics, Vol. I, Wiley-Interscience, 560 pp.

Dutton, J. A., 1976: The Ceaseless Wind, McGraw-Hill, New York, 579 pp.

Fleming, R. J., T. M. Kaneshige, W. E. McGovern and T. E. Bryan, 1979: The Global Weather Experiment II. The Second Special

Observing Period. Bull. Amer. Meteorol. Soc., 60, 1316-1322.

Gandin, L. S., 1963: Objective Analysis of Meteorological Fields. Gidrometeor. Izd., Leningrad. English translation by Israel Program for Scientific Translations, Jerusalem, 1965. [NTIS N6618047, Library of Congress QC996.G3313.]

Ghil, M., M. Halem and R. Atlas, 1979: Time-continuous assimilation of remote-sounding data and its effect on weather forecasting. Mon. Wea. Rev., 107, pp 140-171.

Henrici, P., 1979: Fast Fourier methods in computational complex analysis, SIAM Rev., 21, 484-527.

Hobson, E. W., 1979: The Theory of Spherical and Ellipsoidal Harmonics, Chelsea Publishing, New York, 500.

Kalnay-Rivas, [illegible] and D. Hoitsma, 1979: Documentation of the Fourth Order Band Model, NASA Tech. Memo. 80608, NASA Goddard Space Flight Center, Greenbelt, Maryland 10771.

Kleijnen, J. P. C., 1974: Statistical Techniques in Simulation, Part I, Marcel Dekker, New York, 285.

McPherson, R. D. , K. H. Bergman, R. E. Kistler, G. E. Rasch and D. S. Gordon, 1979: The NMC operational global data assimilation system, Mon. Wea. Rev., 107, 1445-1461.

Pedlosky, J., 1979: Geophysical Fluid Dynamics, Springer-Verlag, New York/Heidelberg/Berlin, 624

Phillips, N. A., 1973: Principles of Large-Scale Numerical Weather Prediction, in Dynamic Meteorology, P. Morel (ed.), E. Reidel Publ., Dordrecht/ Boston, 3-90.

Rutherford, I. D., 1972: Data assimilation by statistical interpolation of forecast error field, J. Atmos. Sci., 29, 809-815.

Swarztrauber, P., and R. Sweet, 1975: Efficient FORTRAN subprograms for the solution of elliptic partial differential equations, NCAR Technical Note TN/IA-109, National Center for Atmospheric Research, Boulder, CO 80307, 139.

Thiébaux, H. J., 1977: Extending estimation accuracy with anisotropic interpolation, Mon. Wea. Rev., 105, 691-699.

Wahba, G., 1979: Spline interpolation and smoothing on the sphere. Tech. Rep. No. 584, Dept. of Statistics, Univ. of Wisconsin, Madison, WI 53706, 38.

Table 1. Test of our extended fast Poisson solver.

Trial function $\phi(\theta,\lambda)$	Form of forcing function	C	M	N	Max$\lvert\phi\rvert$	Max$\lvert\phi_n - \phi\rvert$
$\cos^2\theta\ \cos\lambda$	analytic	$-\sin^2\theta$	16	32	1	8.16 -2
"	"	"	32	64	1	2.3 -2
"	"	$-3.6 + 7$	16	32	1	8.3 -8
"	"	-10.0	16	32	1	3.57 -2
"	finite difference	$-\sin^2\theta$	32	64	1	2.9 -12
$\frac{-\cos^2\theta\ \cos 3\lambda}{48}$	analytic	"	64	128	0.02	7.19 -3
$\cos\phi\ \cos^2\theta$	"	$-10\ \sin^2\theta$	32	64	1	1.18 -2
"	"	$-5\ \sin^2\theta$	32	64	1	1.36 -2
"	"	$-\sin^2\theta$	32	64	1	2.3 -2
$(\sin\theta\ \sin\lambda \cdot \cos^2\theta\ \cos\lambda)$	"	"	32	64	≤ 0.25	9.14 -4

The RHS of (4.2) corresponding to a given trial function was computed either as grid point values of the residual of that function (4.1) ("analytically") or as the residual of that function in (4.2) ("finite-difference"). M is the number of grid intervals into which the meridional coordinate θ was divided; N is the number of grid points in the longitudinal direction. A number a.b + c means (a.b) x 10^{+c}.

Table 2. Forecast fields from the DST-6 experiment S2a (GHA) which were available for our computations.

Date	12h	24h	36h	48h	60h	72h
Feb.						
1						
3	*	*	*	*		
5	*	*	*	*	*	*
7						
9	*	*	*	*	*	*
11						
13	*	*	*	*		
15	*	*	*	*	*	*
17						
19	*	*	*	*		
21	*	*	*	*		
23	*	*	*	*		
25	*	*				
27	*	*	*	*		
29	*	*	*	*		
March						
2	*	*	*	*		
4	*	*	*	*	*	*

Forecasts were initiated at 0000 GMT on the day indicated in the first column. They were carried out for 72h each, but some of the existing prognostic fields were lost in data storage, transmission or retrieval. The columns in the table indicate the availability of the fields at successive synoptic times for each forecast. NMC objective analysis were available at all of the corresponding synoptic epochs. Beyong 48h there were too few fields available to constitute a statistically valid sample.

Table 3. Comparison between model correlations and correlations of the data fields.

	c_o	$\ell_1(\Delta r)$	$\ell_2(\Delta r)$	$L_1(\Delta r)$	$L_2(\Delta r)$	$\ell_1(r^{(m)})$	$\ell_2(r^{(m)})$
12.15	10	.322	.379	.379	.442	.849	.857
12.14	50	.132	.176	.207	.257	.640	.685
12.13	70	.108	.143	.183	.221	.589	.647
12.12	80	.101	.134	.178	.212	.569	.633
12.11	90	.0967	.129	.175*	.207	.552	.620
12.10	100	.0943	.126	.176	.206*	.536	.609
12.9	110	.0938*	.125*	.180	.208	.522	.599
12.8	120	.0946	.125*	.185	.213	.510	.590
12.7	140	.0981	.130	.201	.226	.488	.575
12.6	160	.103	.136	.219	.242	.470	.562
12.5	170	.106	.140	.229	.252	.462	.556
12.4	180	.108	.144	.239	.261	.455	.550
12.1	190	.111	.147	.248	.270	.448	.545
12.2	230	.122	.162	.289	.307	.424	.528
12.3	270	.133	.176	.329	.342	.405	.515
24.8	140	.0745	.0986	.153*	.172	.488	.575
24.7	150	.0744*	.0970	.155	.171*	.479	.568
24.6	160	.0748	.0965*	.159	.172	.470	.562
24.5	170	.0756	.0968	.163	.174	.462	.556
24.4	180	.0768	.0978	.169	.178	.455	.550
24.1	190	.0784	.0994	.174	.182	.448	.545
24.2	230	.0860	.109	.203	.206	.424	.528
24.3	270	.0939	.120	.232	.234	.405	.515

Table 3. (Continued)

	c_o	$\ell_1(\Delta r)$	$\ell_2(\Delta r)$	$L_1(\Delta r)$	$L_2(\Delta r)$	$\ell_1(r^{(m)})$	$\ell_2(r^{(m)})$
36.6	160	.0898	.114	.191*	.203	.470	.562
36.5	170	.0891*	.112	.193	.202*	.462	.556
36.4	180	.0888	.112*	.195	.203	.455	.550
36.1	190	.0889	.112	.199	.205	.448	.545
36.2	230	.0918	.115	.217	.218	.424	.528
36.3	270	.0965	.123	.239	.238	.405	.515
48.6	160	.0952	.123	.202*	.219	.470	.562
48.5	170	.0937	.120	.203	.216	.462	.556
48.4	180	.0928	.117	.204	.213	.455	.550
48.1	190	.0923*	.116	.206	.212*	.448	.545
48.2	230	.0928	.113*	.219	.214	.424	.528
48.3	270	.0951	.116	.235	.226	.405	.515
24/36.8	140	.0808	.104	.166	.182	.488	.575
24/36.7	150	.0792	.102	.165*	.179	.479	.568
24/36.6	160	.0786	.0999	.167	.178*	.470	.562
24/36.5	170	.0785*	.0991*	.170	.178*	.462	.556
24/36.4	180	.0786	.0991*	.173	.180	.455	.550
24/36.1	190	.0791	.0996	.177	.183	.448	.545
24/36.2	230	.0830	.106	.196	.200	.424	.528
24 36.3	270	.0887	.115	.219	.224	.405	.515

The first column indicates the label of the numerical experiment, based on the data set and on the value of c_o used. The data sets are identified by the length of the forecasts on which they were based: 12h, 24h, 36h, 48h or combined 24h and 36h. The second column gives the value of c_o. The next four columns contain the various norms of the difference Δr between model and data correlations (Eqs. (7.1) and (7.2)). These columns contain a star next to the minimum value of each error measure for the corresponding column and data set. The values of c_o which correspond to the largest number of stars in their own row and in the two adjacent rows are boxed. The last two columns give the norms of the model correlations themselves.

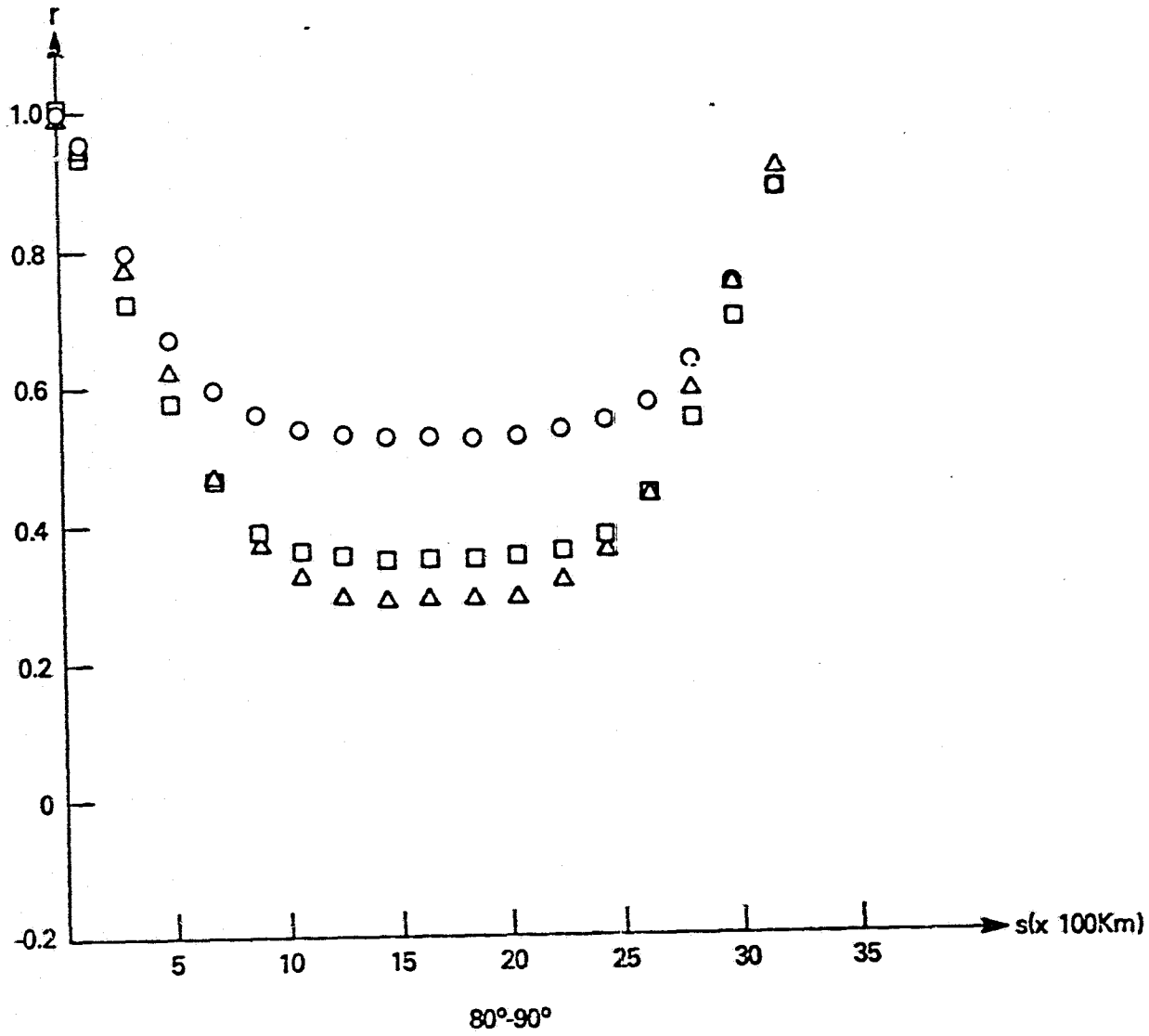

Fig. 1a

Fig. 1a – i. Comparison of model correlations and data correlations. The data were based on both 24h and 36h forecast fields and on NMC analyses; they are given separately for the Northern Hemisphere (Δ) and for the Southern Hemisphere (□). The data for 24h and 36h forecasts seemed sufficiently similar and we used both in order to obtain a larger sample. The model correlations (o) used c_o = 170. Figs. 1a-1i give the correlations for a 10° latitude zone each.

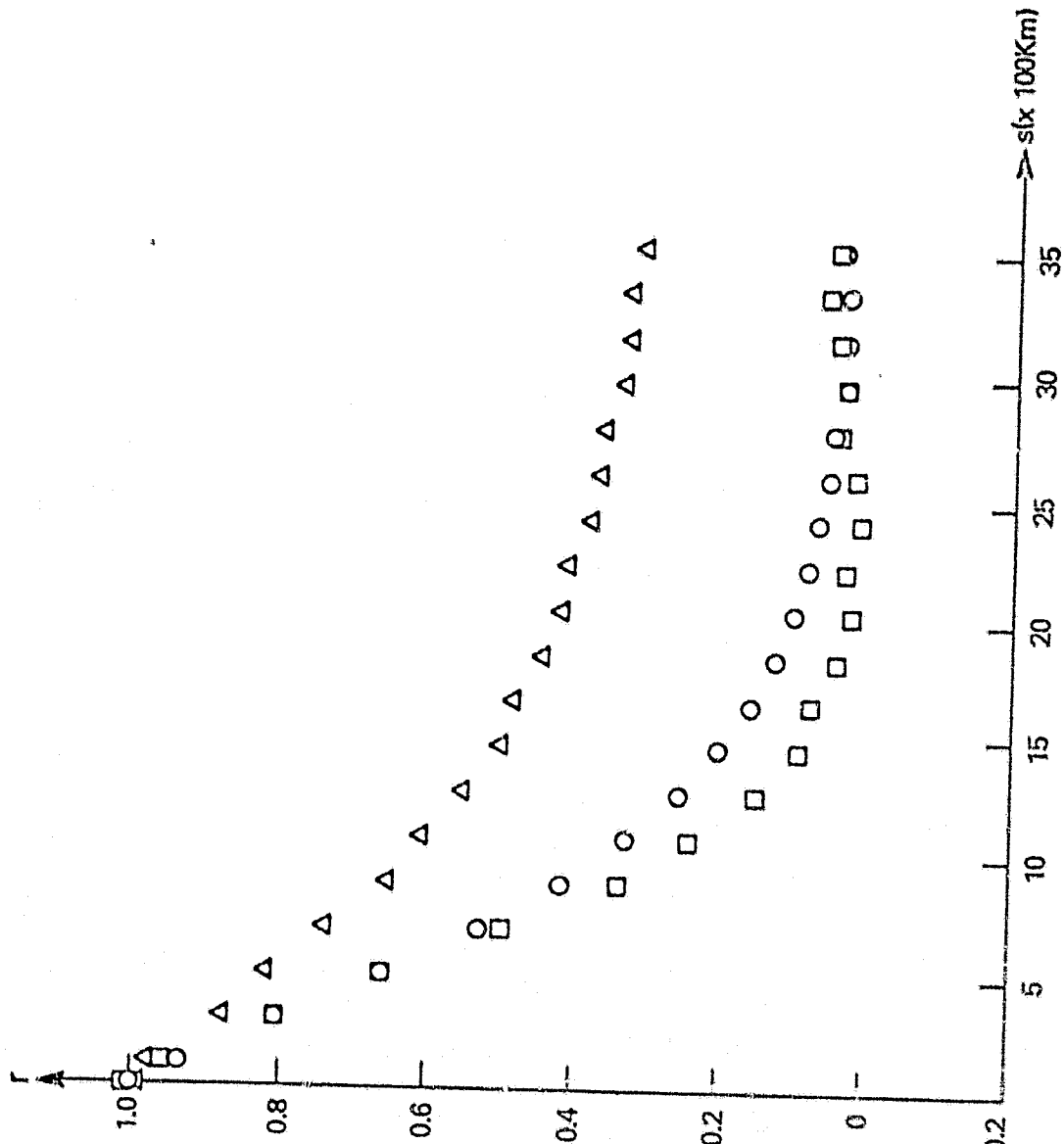

Fig. 1b

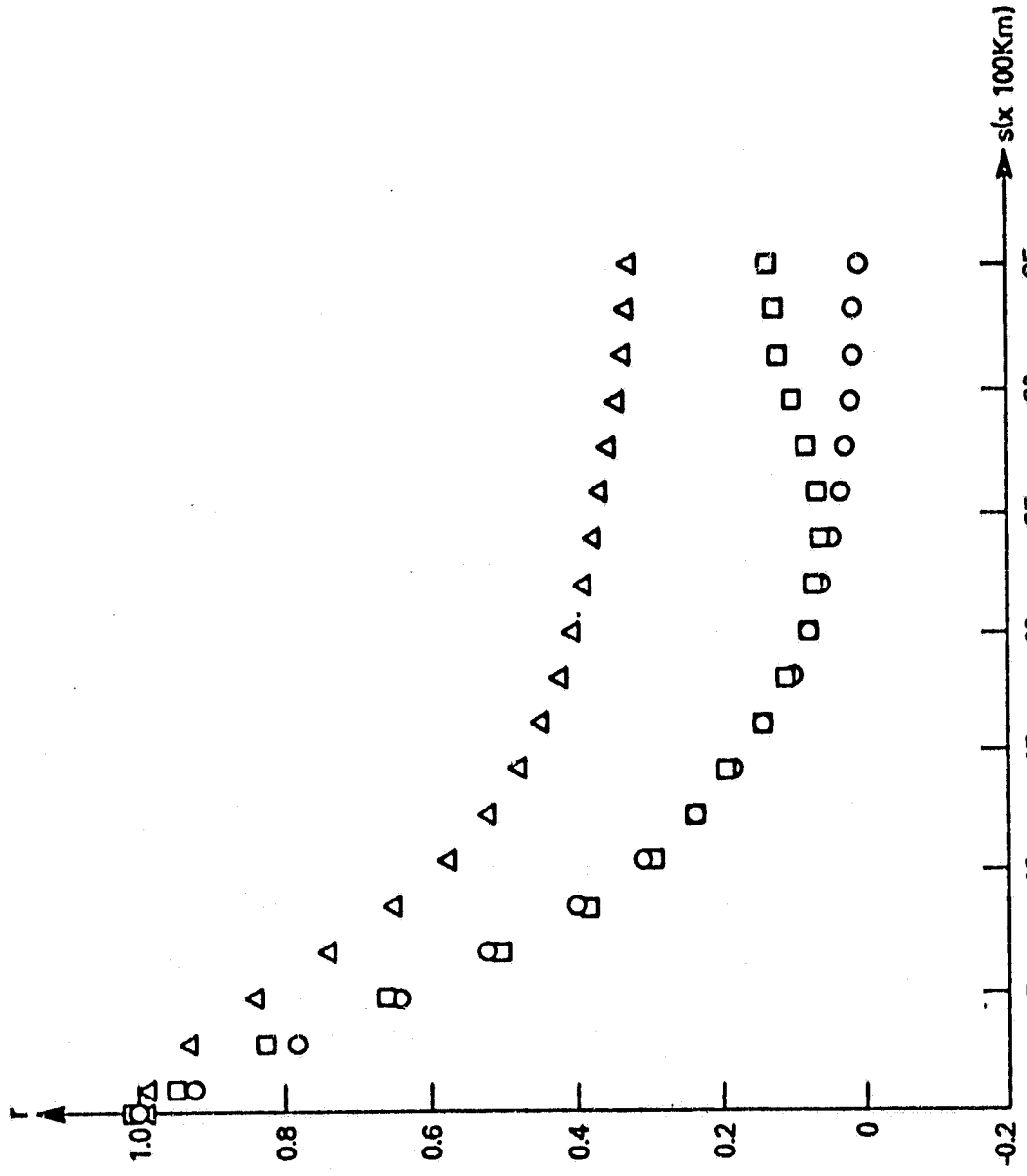

Fig. 1c

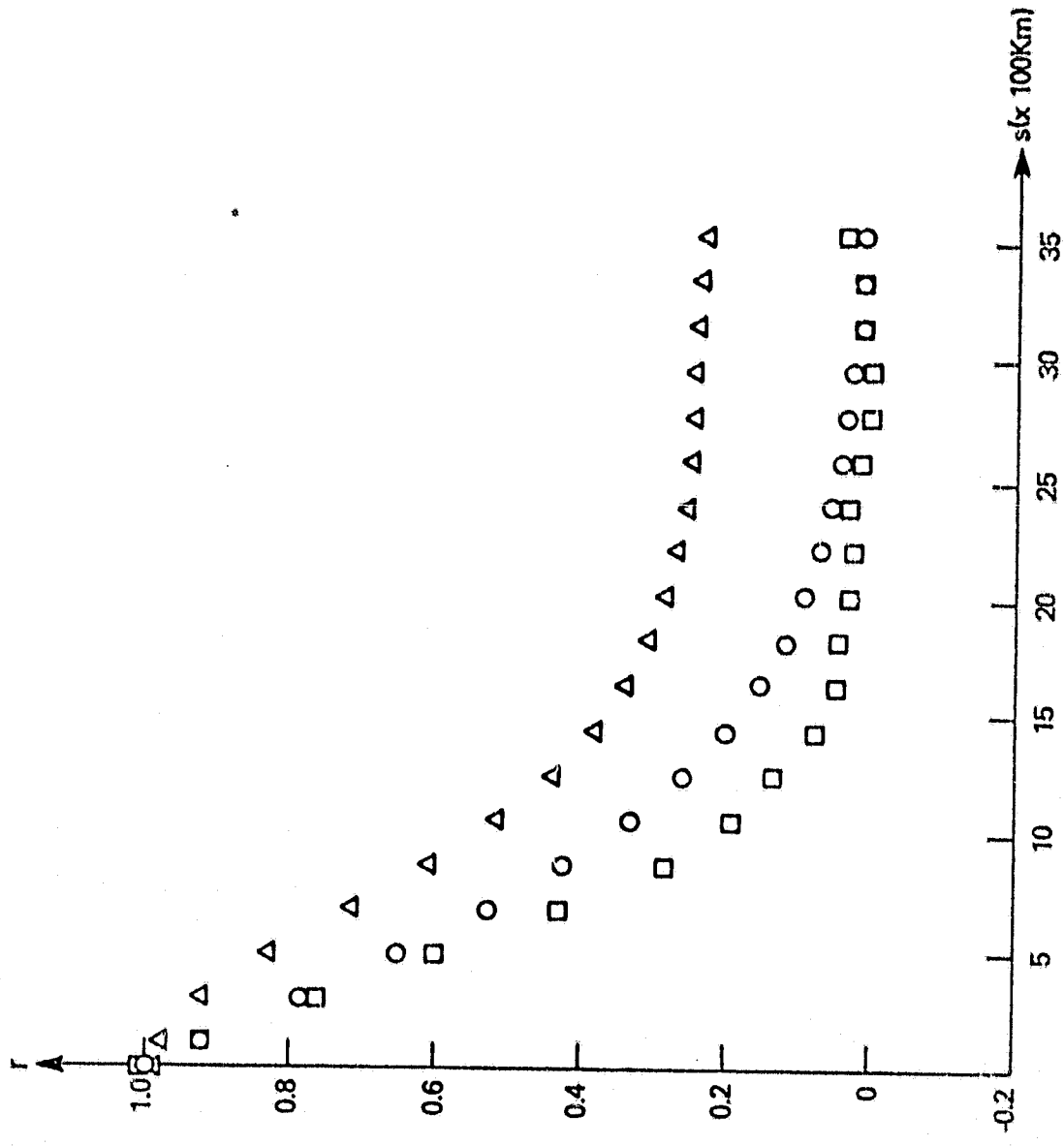

Fig. 1d

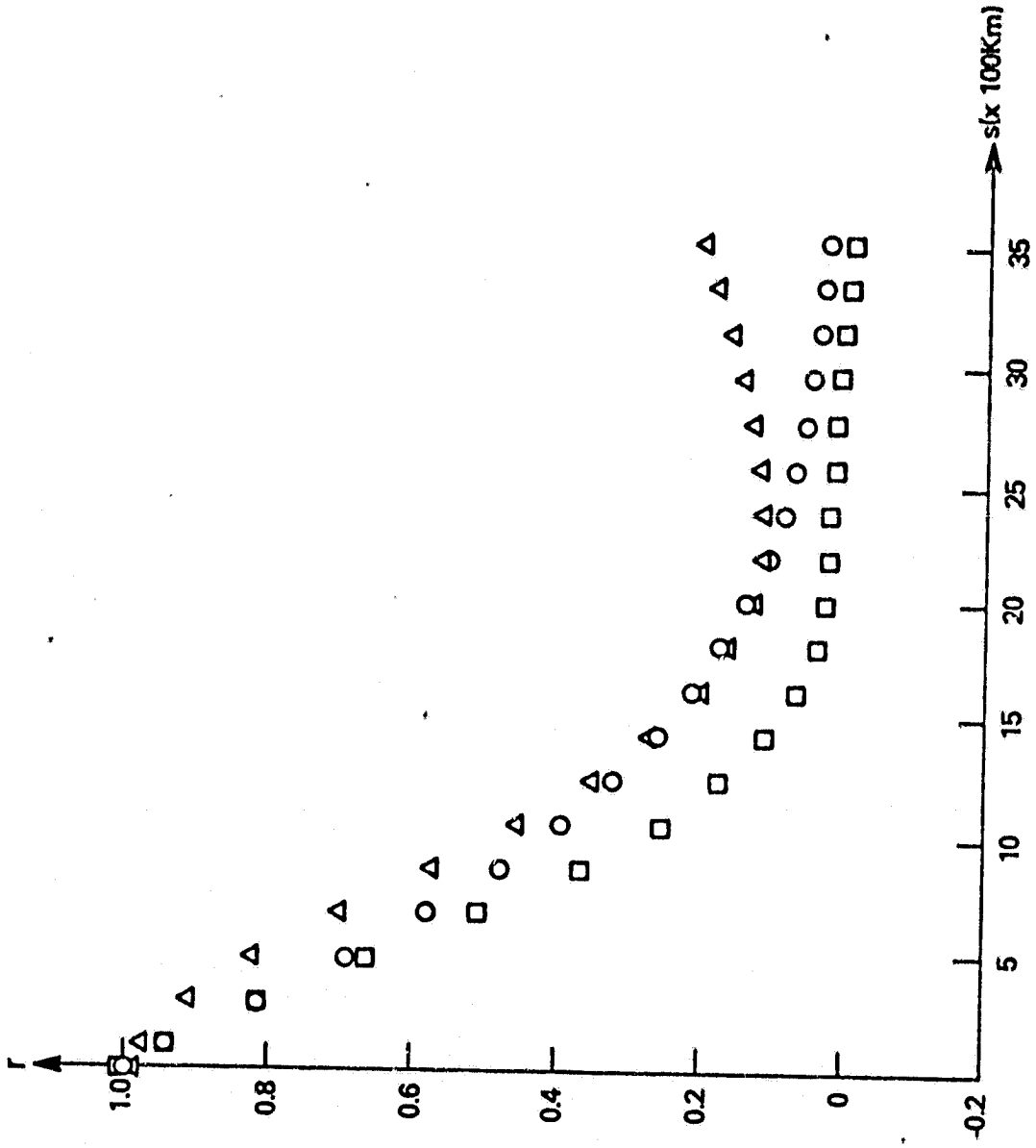

Fig. 1e

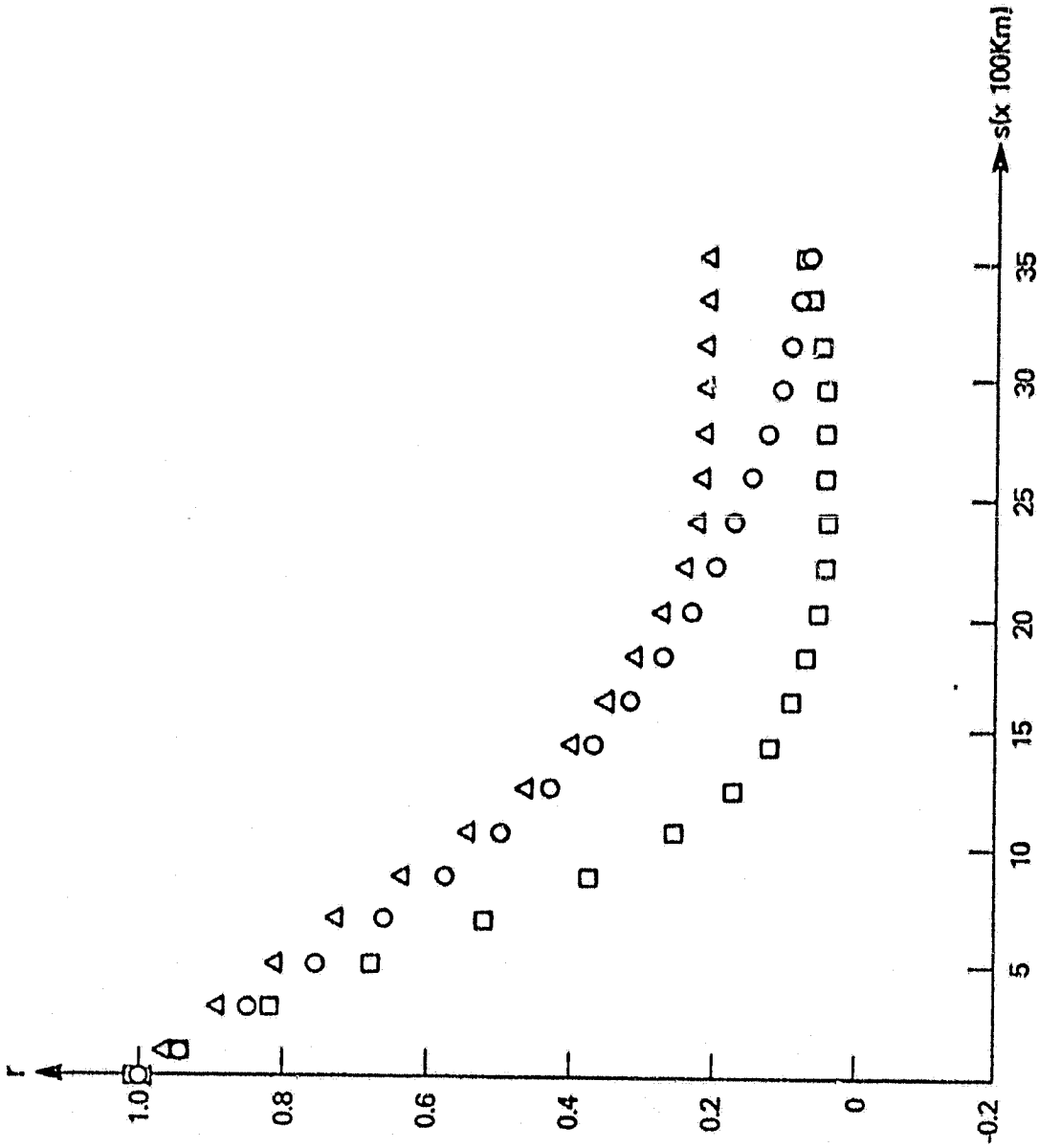

Fig. 1f

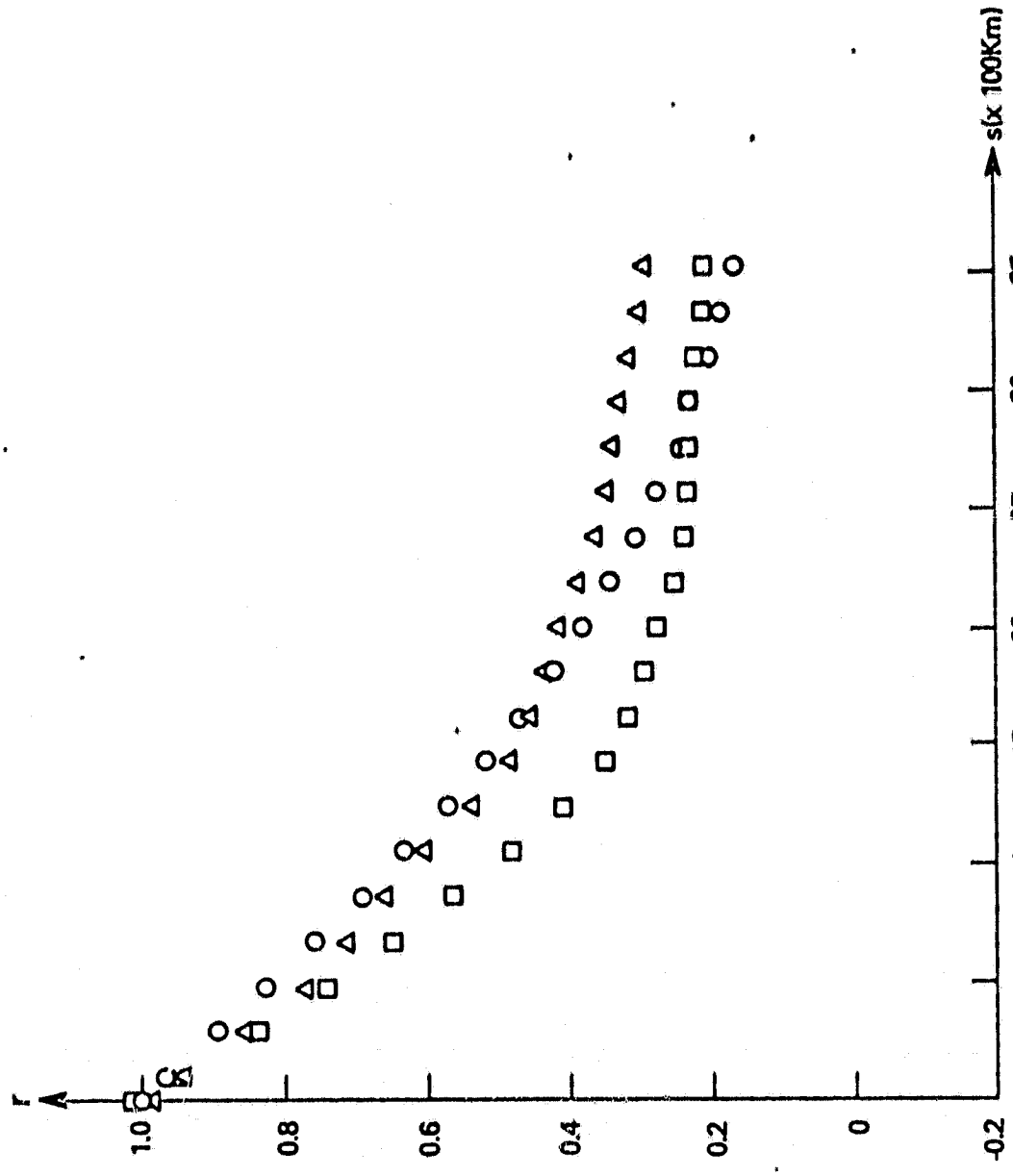

Fig. 1g

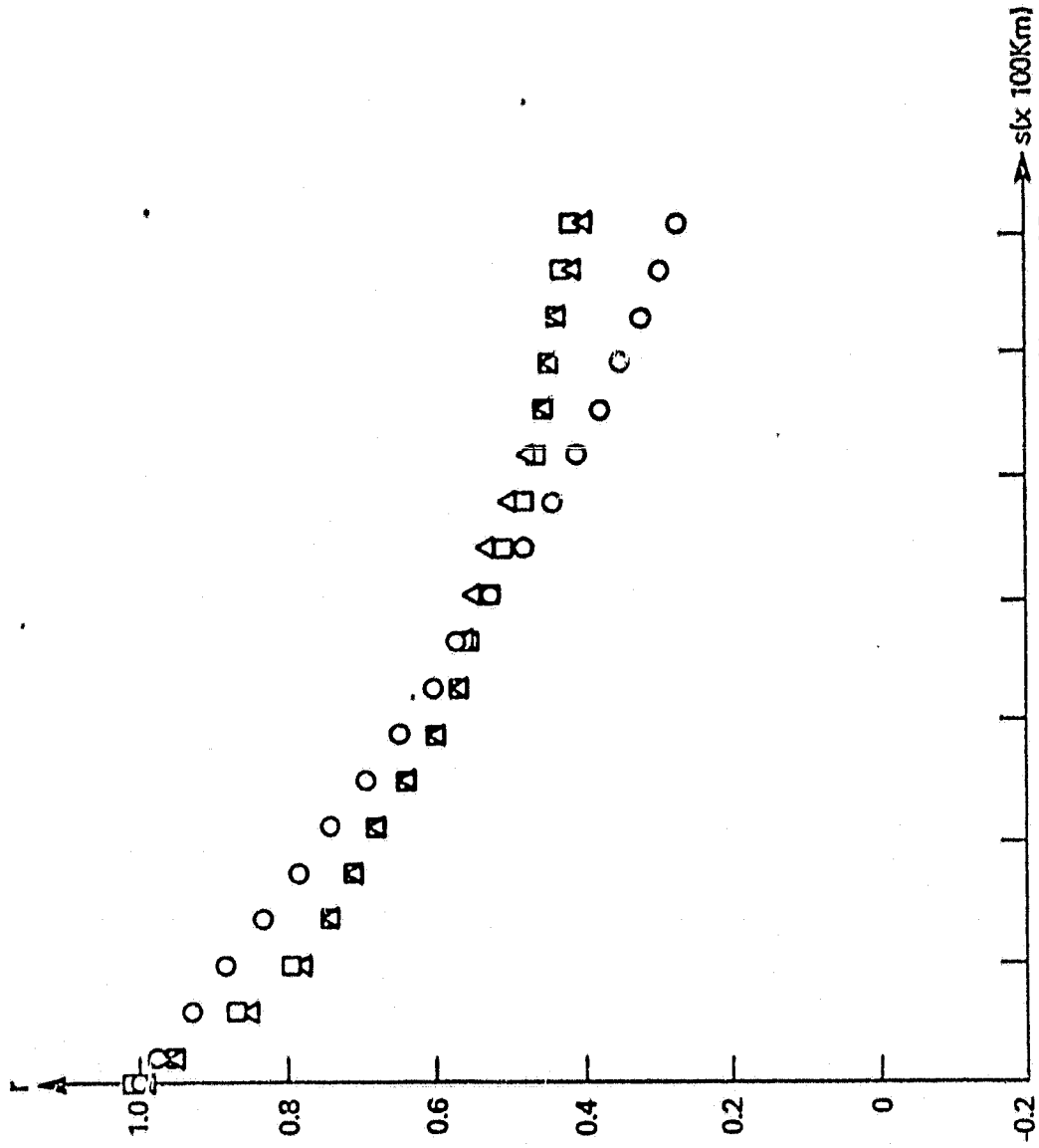

10°-20°

Fig. 1h

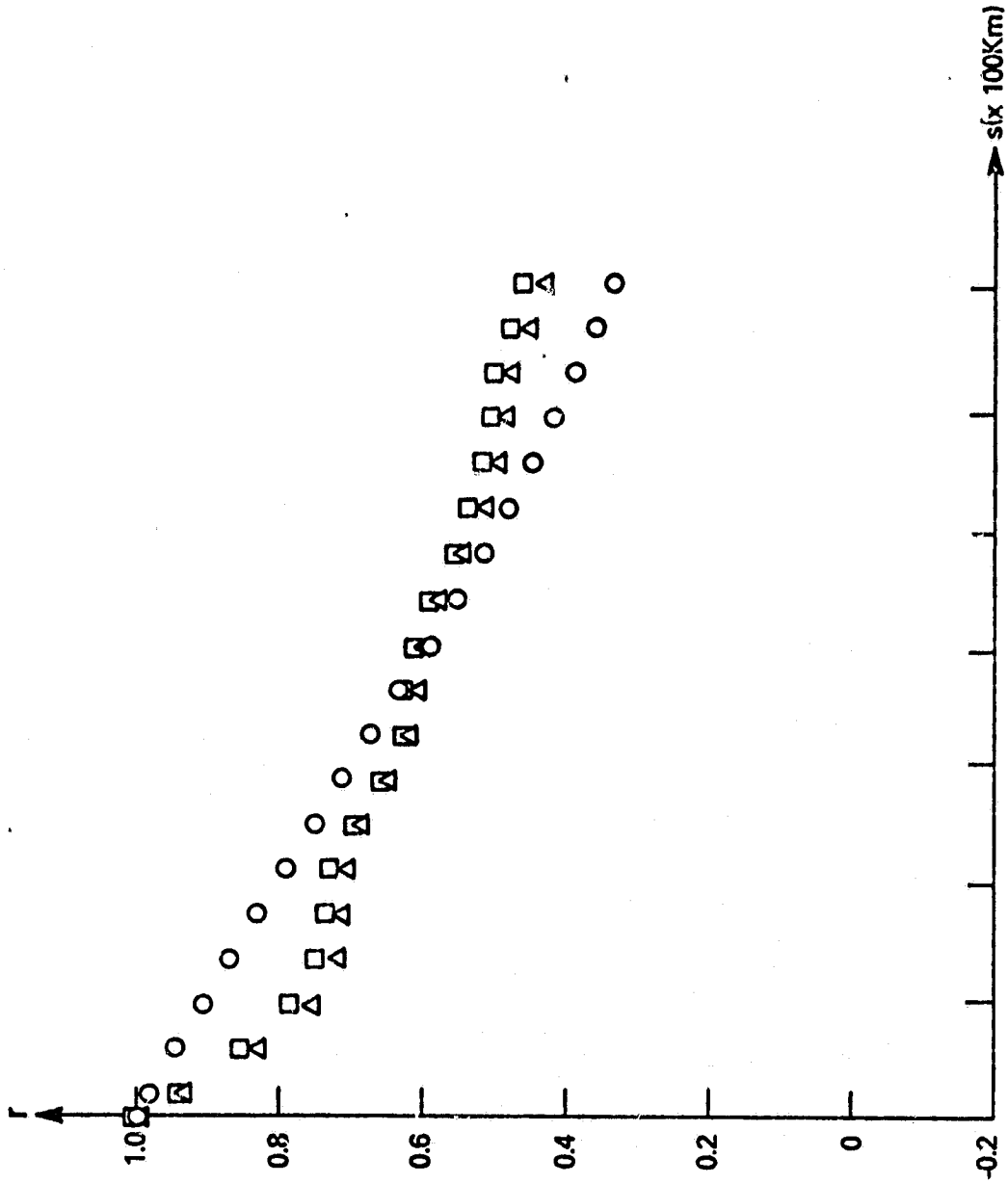

Fig. 11

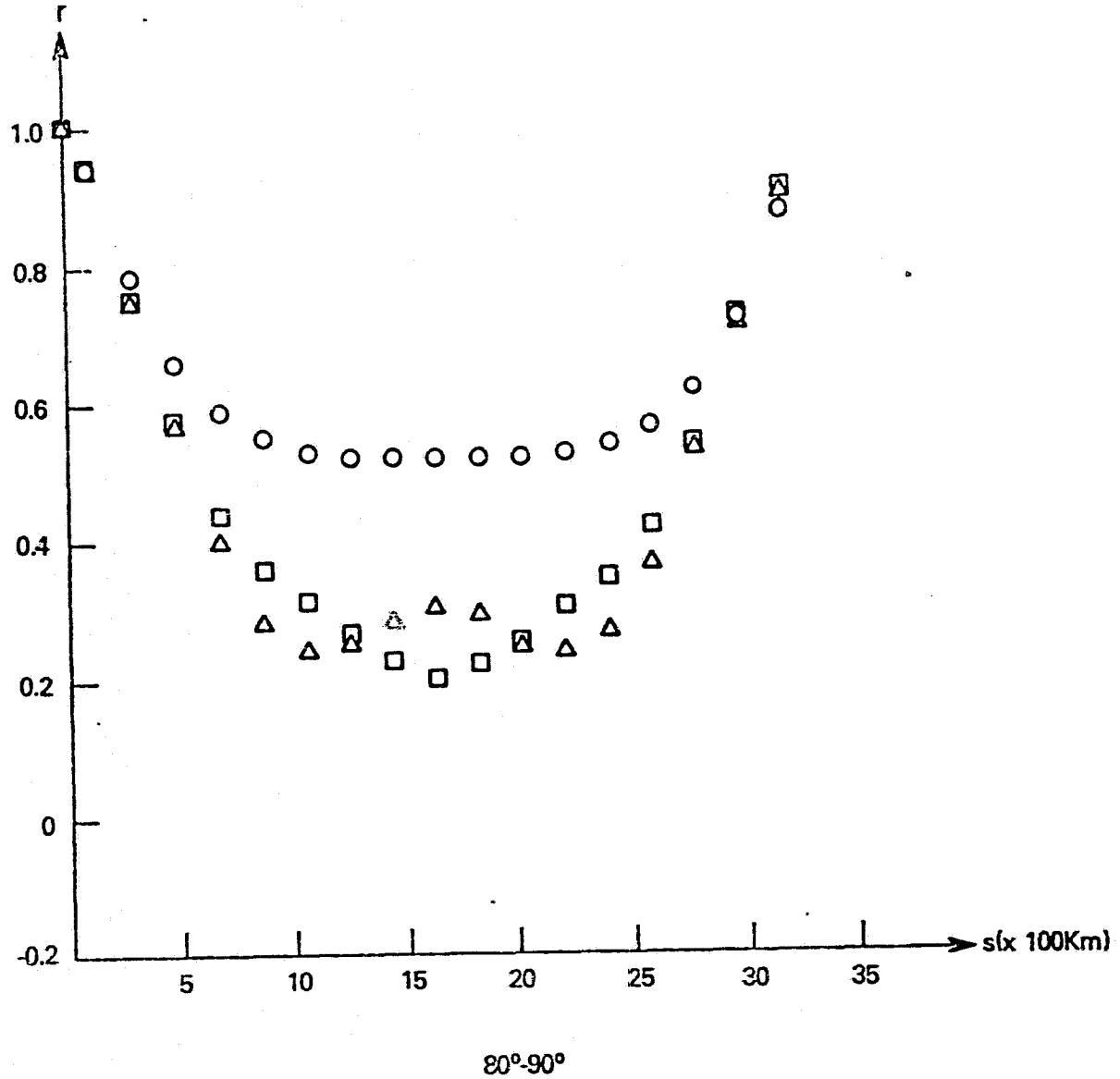

Fig. 2a

Fig. 2a—e. Comparison of model and data correlations. Data are based on 48h forecasts and on the corresponding analyses. Model results used c_o = 190. The symbols are the same as in Fig. 1. Only a number of zones were chosen in order to exhibit differences from the data or results in Fig. 1; these are given in Figs. 2a-2e.

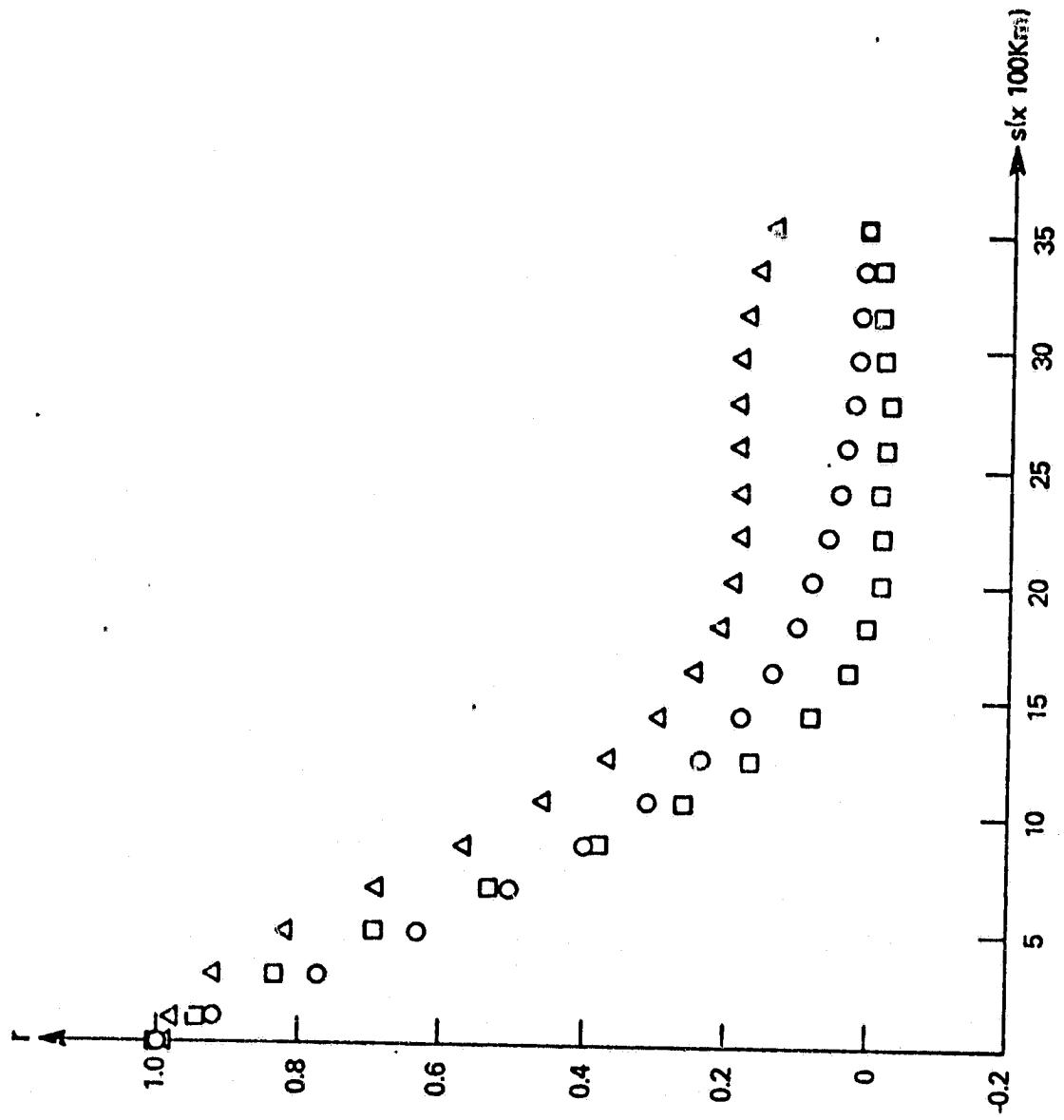

Fig. 2b

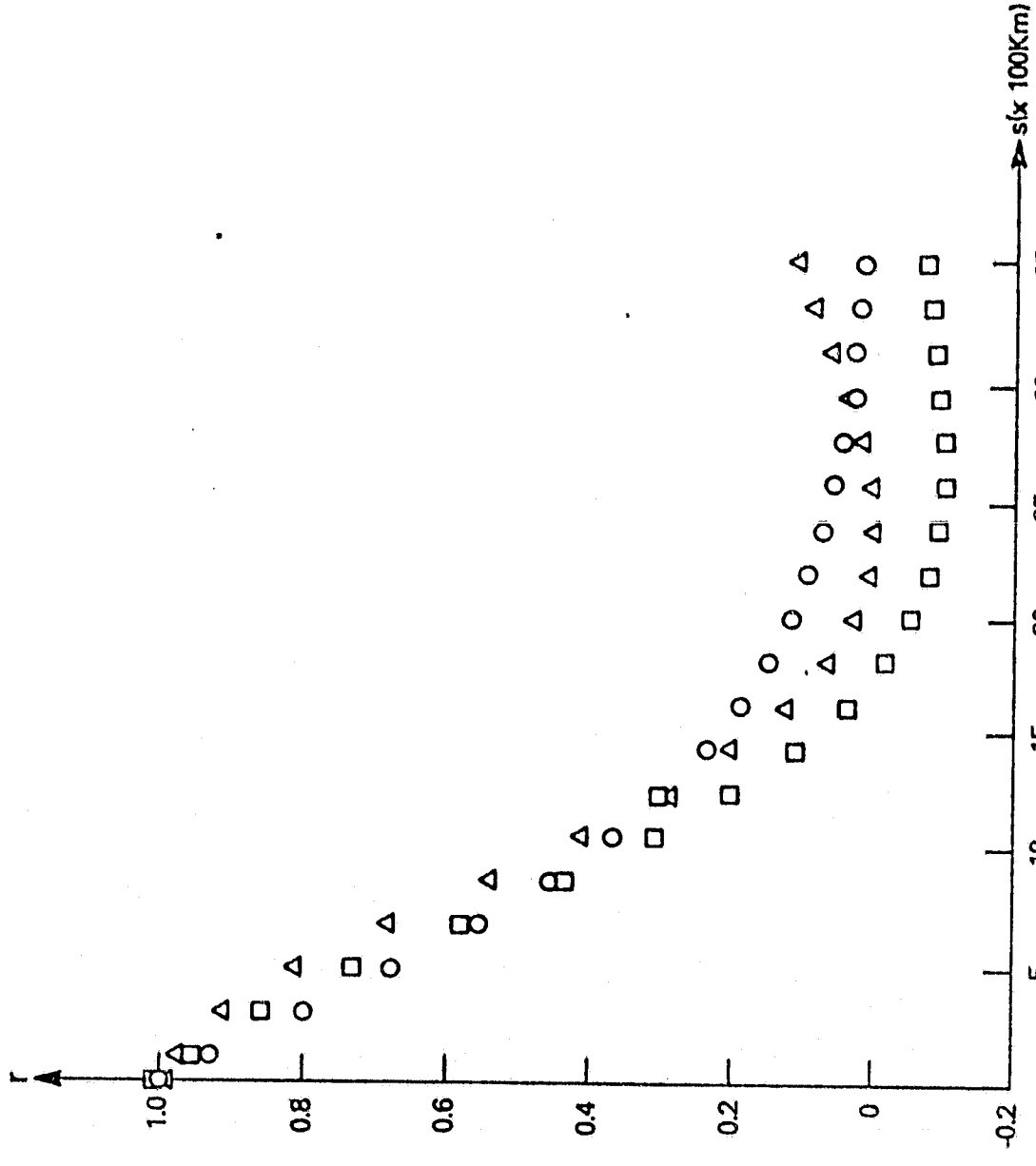

Fig. 2c

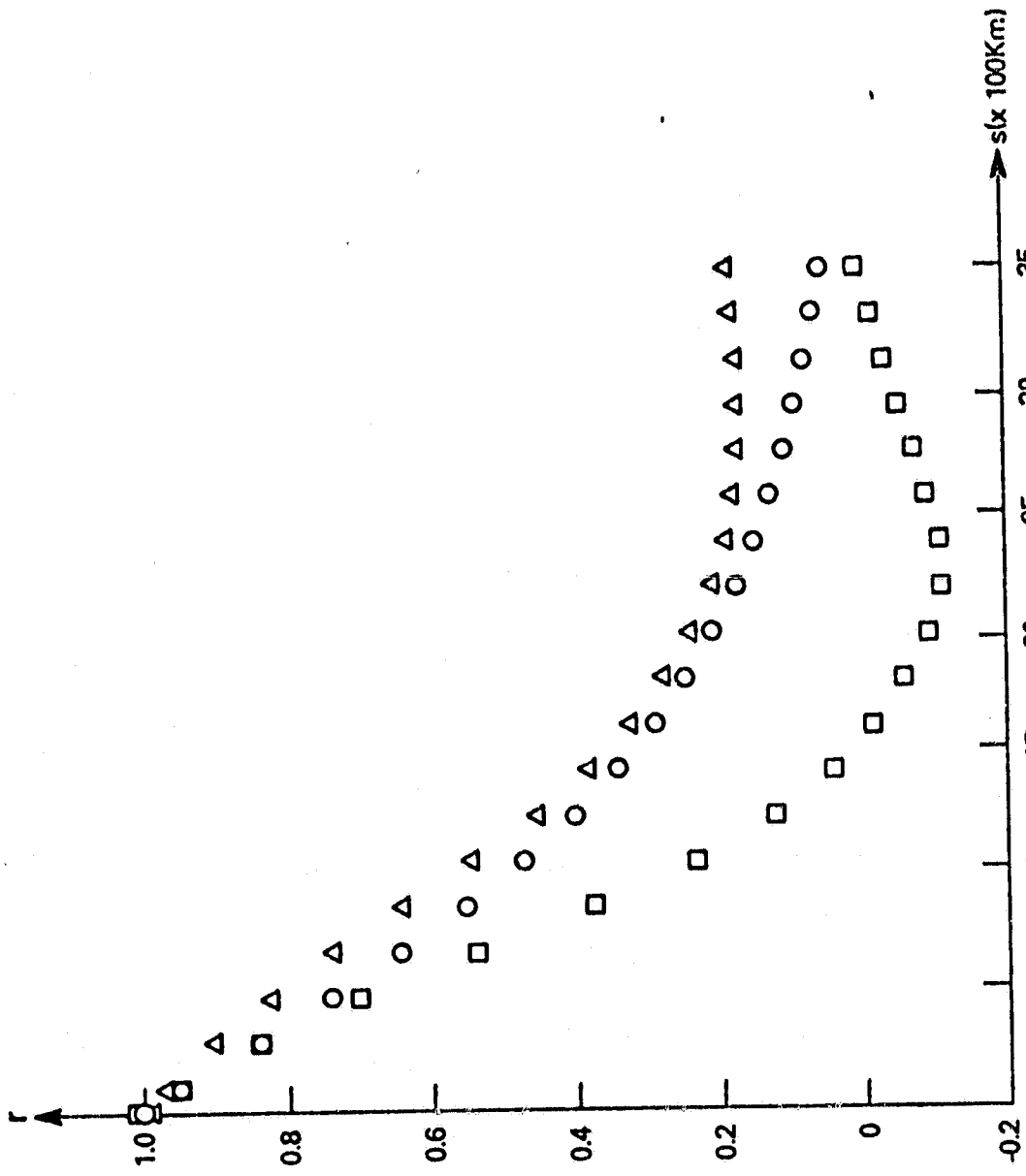

Fig. 2a

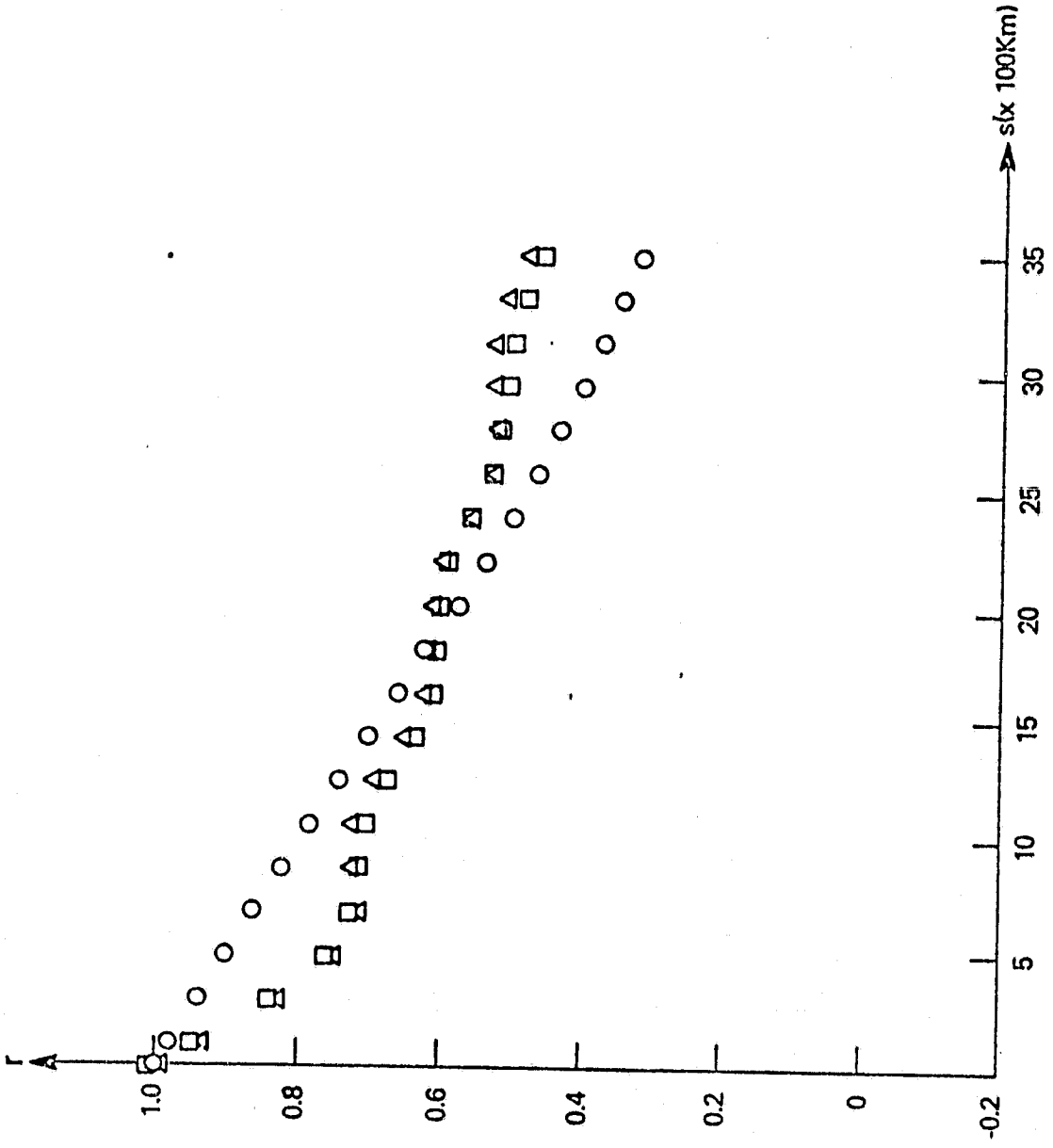

0°-10°

Fig. 2e